Measles skin rash: infection of lymphoid and myeloid cells in the dermis precedes viral dissemination to keratinocytes in the epidermis

The pathogenesis of measles skin rash

Brigitta M. Laksono[1], Paola Fortugno[2], Bernadien M. Nijmeijer[3], Rory D. de Vries[1], Sonia Cordisco[2,#a], Stefan van Nieuwkoop[1], Thijs Kuiken[1], Teunis B. H. Geijtenbeek[3], W. Paul Duprex[4], Francesco Brancati[2,#a], Rik L. de Swart[1]*

[1]Department of Viroscience, Erasmus MC, 3015 CN Rotterdam, the Netherlands

[2]Laboratory of Molecular and Cell Biology, Istituto Dermopatico dell'Immacolata, IDI-IRCCS, 00167 Rome, Italy

[3]Department of Experimental Immunology, Amsterdam Infection and Immunity Institute, Amsterdam University Medical Centres, University of Amsterdam, Amsterdam, the Netherlands

[4]Centre for Vaccine Research, University of Pittsburgh School of Medicine, Pennsylvania, United States of America

[#a] Current address: Department of Life, Health and Environmental Sciences, University of L'Aquila, L'Aquila, Italy

*Correspondence to: Dr. Rik L. de Swart, Department of Viroscience, Erasmus MC. Wytemaweg 80, 3015 CN Rotterdam, The Netherlands. T: +31 10 7044280; F: +31 10 7044760; E: r.deswart@erasmusmc.nl

Abstract

Measles is characterised by fever and a maculopapular skin rash, which is associated with immune clearance of measles virus (MV)-infected cells. Histopathological analyses of skin biopsies from humans and non-human primates (NHPs) with measles rash have identified MV-infected keratinocytes and mononuclear cells in the epidermis, around hair follicles and near sebaceous glands. Here, we address the pathogenesis of measles skin rash by combining data from experimentally infected NHPs, *ex vivo* infection of human skin sheets and *in vitro* infection of primary human keratinocytes. Longitudinal analysis of the skin of experimentally MV-infected NHPs demonstrated that infection in the skin precedes onset of rash by several days. MV infection was initiated in lymphoid and myeloid cells in the dermis before dissemination to the epidermal keratinocytes. These data were in good concordance with *ex vivo* MV infections of human skin sheets, in which dermal cells were more targeted than the epidermal ones. To address viral dissemination to the epidermis and to determine whether the dissemination is receptor-dependent, we performed experimental infections of primary keratinocytes collected from healthy or nectin-4-deficient donors. These experiments demonstrated that MV infection of keratinocytes is nectin-4-dependent, and nectin-4 expression was higher in differentiated than in proliferating keratinocytes. Based on these data, we hypothesise that measles skin rash is initiated by migrating MV-infected lymphocytes that infect dermal skin-resident $CD150^{+}$ immune cells. The infection is subsequently disseminated from the dermal papillae to $nectin\text{-}4^{+}$ keratinocytes in the basal epidermis. Lateral spread of MV infection is observed in the superficial epidermis, most likely due to the higher level of nectin-4 expression on differentiated keratinocytes. Finally, MV-infected cells are cleared by infiltrating immune cells, causing hyperaemia and oedema, which give the appearance of morbilliform skin rash.

48

Author Summary

50 Several viral infections are associated with skin rash, including parvovirus B19, human
51 herpesvirus type 6, dengue virus and rubella virus. However, the archetype virus infection
52 that leads to skin rash is measles. Although all of these viral exanthemata often appear similar,
53 their pathogenesis is different. In the case of measles, the appearance of skin rash is a sign
54 that the immune system is clearing MV-infected cells from the skin. How the virus reaches
55 the skin and is locally disseminated remains unknown. Here we combine observations and
56 expertise from pathologists, dermatologists, virologists and immunologists to delineate the
57 pathogenesis of measles skin rash. We show that MV infection of dermal myeloid and
58 lymphoid cells precedes viral dissemination to the epidermal keratinocytes. We speculate
59 that immune-mediated clearance of these infected cells results in hyperaemia and oedema,
60 explaining the redness of the skin and the slightly elevated spots of the morbilliform rash.

61

Introduction

Measles virus (MV) is a highly contagious enveloped virus with a negative single-stranded RNA genome, that belongs to the family *Paramyxoviridae*, genus *Morbillivirus* (PMID: 31609197). Measles is associated with fever, cough and a characteristic maculopapular skin rash [1]. MV utilises two cellular receptors to infect its target cells: CD150 and nectin-4 [2-4]. CD150 plays a crucial role during viral entry and systemic dissemination. It is expressed on subsets of immune cells, including macrophages, dendritic cells (DCs) and lymphocytes. Nectin-4 is crucial for viral transmission to the next host. It is an adherens junction protein expressed at the basolateral surface of differentiated respiratory epithelial cells and is involved in the maintenance of epithelium integrity [5, 6].

Following entry of MV into the respiratory tract, the primary infection of myeloid cells leads to a cell-associated viremia mediated by $CD150^+$ lymphocytes, resulting in systemic disease [7-9]. During a clinically silent incubation phase of 7 to 10 days, circulating MV-infected lymphocytes migrate into various tissues and transmit the virus to susceptible tissue-resident $CD150^+$ immune cells and nectin-4^+ epithelial cells. Basolateral infection of respiratory epithelial cells leads to the apical release of nascent virions into the lumen of the respiratory tract [10-12]. Shedding is associated with the onset of prodromal clinical signs such as fever and cough [9, 13]. Maculopapular skin rash and conjunctivitis follow a few days later [9] and are associated with onset of MV-specific cellular immune responses [13]. Patients with a compromised cellular immune system do not develop rash or conjunctivitis, but are at high risk of developing severe disease [14].

In histopathological studies of human skin biopsies, measles skin rash is mostly characterised by infection and necrosis of keratinocytes and mononuclear cells in the epidermis, and multinucleated giant cells located in proximity to hair follicles and sebaceous glands [15, 16]. It has been postulated that measles rash starts by infection of dermal endothelial cells [17]. However, these cells neither express CD150 nor nectin-4 [18, 19]. Moreover, we have previously identified MV-infected lymphocytes and DCs in the skin of experimentally infected non-human primates preceding onset of skin rash [8]. Besides $CD150^+$ and $nectin\text{-}4^+$ cells, other cells that express DC-SIGN or Langerin could play a role in the pathogenesis of measles skin rash, since DC-SIGN and Langerin facilitate attachment, but not entry, of MV and thus potentially help in spreading the infection in the skin.

In order to understand the pathogenesis of measles skin rash, it is important to understand both the architecture of the skin and the spatial organisation of cell subsets that express either CD150 or nectin-4. The dermis is vascularised and contains several subsets of immune cells that express CD150. These include a network of myeloid DCs and clusters of tissue-resident $CD4^+$ and $CD8^+$ T cells [20-22]. In contrast to the dermis, the epidermis is not vascularised. It mainly consists of keratinocytes, with an interdigitating network of Langerhans cells (LCs) and melanocytes [23]. The epidermis comprises of proliferating keratinocytes at the basal lamina that differentiate towards the skin surface. Keratinocytes express nectin-4 and expression levels increase during differentiation. It is known that keratinocytes are susceptible to MV infection [24]. The top layer of the epidermis, the stratum corneum, consists of a layer of dead keratinocytes called corneocytes. Interestingly, immune cells and nutrients can only reach the epidermis by migration and diffusion, respectively, from the superficial dermis through the basal lamina. The pilosebaceous unit begins at the

epidermis and extends into the dermis, where the surrounding tissue is usually better vascularised. Therefore, tissue-resident lymphocytes are often seen in close association with these structures [21]. Hair follicles are mainly constituted of keratinocytes that express high levels of nectin-4 explaining their propensity for MV infection [25].

During viraemia, systemic dissemination of MV is mediated by circulating MV-infected $CD150^+$ lymphocytes. However, how these cells infiltrate the skin, ultimately resulting in skin rash, remains largely unknown. In this study we aimed to identify the cells involved in MV infection of the skin and to understand the pathogenesis of skin rash. We demonstrate that MV infection of lymphoid and myeloid cells in the superficial dermis precedes dissemination to epidermal keratinocytes, which is followed by onset of the typical skin rash.

Results

MV skin infection precedes onset of rash in experimentally-infected non-human primates (NHPs)

We retrospectively analysed data from cynomolgus macaques (*Macaca fascicularis*) inoculated with recombinant MV (rMV) strains expressing enhanced green fluorescent protein (EGFP) [26]. Fluorescent spots, indicating the presence of MV-infected cells, became detectable in the skin around 8 days post-inoculation (dpi), although skin rash only became prominent between 11 and 13 dpi (Fig 1) [27]. We previously reported that by 9 dpi, *i.e.* before the onset of rash, infected cells in the skin mainly consisted of $EGFP^+$ lymphocytes and DCs [8].

Infection of dermal immune cells precedes infection of epidermal keratinocytes in experimentally-infected NHPs

We performed immunohistochemistry on formalin-fixed and paraffin-embedded skin samples from these NHPs and showed co-localisation of EGFP and MV nucleoprotein (N) signals in sequential skin sections, which indicated the presence of MV-infected cells. At 9 dpi, the infected cells were predominantly located in the superficial dermis, most especially around the hair follicles and sebaceous glands (Fig 2a – f). Most infection in the epidermis appeared as single-cell infection near dermal papillae and later progressed into multiple-cell infection and syncytia (Fig 2g – i) between 9 and 11 dpi. This epidermal infection later reached the superficial side at 13 dpi, by which time the infection in the dermis already had been cleared. Oedema and spongiosis could be observed at this time point.

To identify the phenotype of the infected cells, we performed dual-indirect immunofluorescence (IIF) on these sequential skin sections (Fig 3). $CD45^+$ white blood cells were present in the superficial dermis, most especially in or around blood vessels, hair follicles and sebaceous glands and, to a lesser degree, in the epidermis. Some of these $CD45^+$ white blood cells were $CD3^+$ T cells that were located in the reticular dermis, while some others were S100A8/A9-complex$^+$ (Mac387) macrophages that were abundantly present in the superficial dermis, most especially in or around the blood vessels, hair follicles or sebaceous glands. Cytokeratin$^+$ cells were restricted to the epidermis and pilosebaceous units. In contrast, $CD31^+$ endothelial cells of the blood vessels were restricted to the dermis.

MV-$EGFP^+$ cells could be found as early as 9 dpi in the dermal papillae. These cells predominantly belonged to the white blood cell phenotype (Fig 3a), which were mostly T cells or macrophages (Fig 3b – c). Some MV-infected cells were present in or surrounding blood vessels (Fig 3d). In some areas in which the infection was more progressed, the infection spread to the epidermis, even into the most superficial layers, which comprised of differentiated keratinocytes (Fig 3e). The MV-infected white blood cells were still detectable in the dermis on day 11, sometimes in close proximity with uninfected white blood cells, mostly macrophages (Fig 3f – h). These cells clustered close to the dermal papillae, where a lot of blood vessels could be found (Fig 3i). Meanwhile, the infection in the epidermis had progressed laterally and apically (Fig 3j). We also observed keratinocytes at the site of infection expressing S100A8/A9 complex (Fig 3h) as a response to inflammatory stimuli. By 13 dpi, the dermis was almost clear of the infected cells and was filled with white blood cell infiltrates, mostly macrophages (Fig 3k – m). No MV-infected endothelial cells were observed

166 at this time point (Fig 3n). Infection in the epidermis had mostly resolved, although remaining
167 infected follicular keratinocytes could still be detected (Fig 3o).
168
169 Focal MV skin infection, in which the progression of infection was different in different sites,
170 was observed as early as 9 dpi. More infected cells were observed in the dermis and epidermis
171 in the sites where the infection had progressed further. At the same time point, but in a
172 different site, where the infection has not progressed, individual MV-infected cells were more
173 often found only in the dermis. This suggested that time was not the only important factor in
174 the pathogenesis of MV skin rash. The location in which MV-infected cells could be found and
175 the interaction with surrounding cells could also play a crucial role in establishing infection in
176 the skin. We observed MV-infected white blood cells in dermal papillae or close to the basal
177 epidermis (Fig 4a). MV-infected T cells, although could often be found near the dermal
178 papillae around 9 and 11 dpi, became scarce at 13 dpi and could only be observed in the
179 reticular dermis. At this late time point, the MV-infected T cells were found surrounded by
180 uninfected T cells (Fig 4b). Close interaction could also be observed among MV-infected cells
181 with HLA-DR$^+$ antigen-presenting cells (APCs), for example through a long, EGFP$^+$ dendrite (Fig
182 4c). We observed MV-infected cells surrounded by or in close proximity to endothelial cells
183 (Fig 4d) at 9 dpi at the site where the infection has progressed further. Very rarely, in the
184 same site, we found MV-infected CD31$^+$ endothelial cells near other infected cells (Fig 4e).
185 We also observed MV-infected cells in the dermis that were negative for white blood cell, APC,
186 endothelial cell and epithelial cell markers and appeared to be spindle- or dendritic-like cells
187 (Fig 4f).
188

In the epidermis, a number of MV-infected white blood cells could be observed since 11 dpi, accompanied by infiltration of uninfected white blood cells to the site of infection (Fig 4g – i). These MV-infected white blood cells were negative for keratinocyte, macrophage and T cell markers, thus most likely to be LCs (Fig 4j – k). These cells were found in close proximity to keratinocytes, which were also positive for MV infection (Fig 4k), although keratinocyte infection could still be detected despite the absence of MV-infected white blood cells in the observed two-dimensional plane (Fig 4l).

Ex vivo MV infection of human skin sheets results in higher infection levels in the dermis than in the epidermis

Based on the observations in NHPs, we hypothesised that infection of immune cells in the dermis plays a major role in the pathogenesis of measles skin rash. To test this hypothesis, we *ex vivo* inoculated human full skin or enzymatically-separated epidermal and dermal sheets with rMV based on a wild-type virus strain Khartoum-Sudan (KS) expressing the fluorescent reporter protein Venus from an additional transcription unit in position 3 of the viral genome (rMV^{KS}Venus(3)). We monitored the infection up to seven days. We observed that Venus^{+} cells could be detected by inverted laser scanning microscopy as early as 2 dpi, with higher infection levels in the dermis than the epidermis (Fig 5a). The phenotype and the percentage of emigrant MV-infected cells from the skin sheet cultures were determined by flow cytometry. These cells turned out to be CD4^{+} T cells, APCs and non-lymphocytes. In accordance to the observation on Venus^{+} cells under the inverted laser scanning microscopy, the percentage of MV-infected cells was higher in the dermis than in the epidermis (Fig 5b). This finding suggested that the dermis is an important site where MV infection is established.

213 Previous studies showed that mature LCs are susceptible to MV infection and Langerin can
214 act as an attachment receptor, but not entry receptor, for the virus [28]. To determine
215 whether LCs play a role in MV epidermal infection as initial target cells, we performed dual-
216 IIF stainings on human epidermal sheets from healthy donors infected with rMV^{KS}Venus(3).
217 We found that despite the abundant presence of LCs in the epidermal sheets, none of these
218 were Venus-positive (S1). This finding suggests that LCs do not play a major role in the
219 pathogenesis of measles skin rash.
220
221 **Human primary keratinocytes are susceptible to *in vitro* MV infection in a nectin-4-**
222 **dependent manner**
223 To investigate the susceptibility and the permissiveness of keratinocytes, we inoculated
224 human primary human keratinocytes derived from two healthy donors or from a patient
225 affected by ectodermal dysplasia-syndactyly syndrome (EDSS1, OMIM 613573), an autosomal
226 recessive disorder caused by mutations in the nectin-4 encoding gene *PVRL4* [25]. In this
227 patient, EDSS is secondary to compound heterozygous mutations c.554C>T and c.906delT in
228 the *PVRL4* gene (family B in [25]). While the first is a missense mutation (p.Thr185Met)
229 affecting a highly conserved residue of nectin-4 located in its second extracellular
230 immunoglobulin-like domain, the second variant leads to a prematurely truncated protein
231 (p.Pro304HisfsX2). Previous study has shown that in cultured epidermal keratinocytes from
232 this EDSS patient, nectin-4 mRNA displayed nearly 50% reduced expression in line with
233 nonsense mRNA decay of the c.906delT allele, suggesting that all the residual protein
234 expressed on the keratinocyte surface (about 10%) is represented by the p.Thr185Met
235 mutant [25]. In agreement with previously published data, nectin-4 expression on the cell
236 surface was highest in differentiated healthy donors' keratinocytes, as demonstrated by flow

237 cytometry. However, differentiation did not result in increase of nectin-4 expression in the
238 EDSS patient's keratinocytes (S2) [25]. To determine whether the proliferating and
239 differentiated keratinocytes were susceptible to MV infection, we inoculated them with two
240 MV strains expressing fluorescent reporter proteins (rMV^{IC323}EGFP(1) or rMV^{KS}Venus(3)) [29]
241 or a strain engineered to be unable to recognise nectin-4 (the 'nectin-4-blind (N4B)' strain
242 rMV$^{KS\text{-}N4b}$EGFP(3)) [10] at a multiplicity of infection (MOI) of 1. After 48 hours, we observed
243 higher frequencies of fluorescent cells in differentiated than in the proliferating cells (Fig 6).
244 Infection of keratinocytes with the nectin-4-blind MV resulted in low numbers of single
245 infected cells. Few MV infected cells were detected in the EDSS proliferating and
246 differentiated cultures.
247
248 To assess whether the infected keratinocytes also produced cell-free virus and were thus
249 capable of spreading the infection, the supernatant of the MV-infected keratinocytes was
250 collected and the titre of cell-free virus in the supernatant was assessed [30]. Cell-free MV
251 was detectable in the culture supernatant of the infected proliferating and differentiated
252 keratinocytes. In healthy donors, virus titres in supernatants of differentiated keratinocytes
253 were higher than those in supernatant of proliferating keratinocytes. Interestingly, virus titres
254 of the EDSS patient's proliferating keratinocytes were comparable to those of the healthy
255 donors (Fig 7a). The difference in virus titres increased as the cells differentiated, since the
256 titre was higher in healthy donors than in the patient.
257
258 Low expression of mutant nectin-4 on the surface of EDSS patient's keratinocytes could
259 apparently still facilitate MV infection, leading to the production of new viral particles by
260 infected keratinocytes, suggesting that the p.Thr185Met mutation in the second

261 immunoglobulin-like domain does not affect the virus binding. To validate this observation,
262 we transiently transfected human embryonic kidney (HEK) 293T cells with a plasmid
263 containing either wild-type or two mutant nectin-4 (p.Thr185Met) insert. The cells were then
264 inoculated directly with rMV^{KS}Venus(3) at an MOI of 3. Infection efficiency was measured by
265 flow cytometry 24 hours post-infection. Expression levels of both wild-type and mutant
266 nectin-4 was comparable and both nectin-4-transfected cells, but not the mock-transfected
267 cells, proved susceptible to MV infection (Fig 7b), which confirmed that the defective nectin-
268 4 (p.Thr185Met) could still function as a cellular receptor for MV.
269
270 Based on our findings, combined with previously published observations, we postulate a
271 model that describes the progression of MV skin infection and the development of measles
272 rash (Fig 8). The model takes viral tropism, location, interaction and motility of the susceptible
273 cells, as well as the virus-specific immune responses into account. MV-infected cells enter the
274 superficial dermis through the blood vessels and spread the infection to the tissue-resident
275 dermal T cells, APCs and spindle- or dendritic-like cells around 7 dpi. The infection progresses
276 several days later to the adjacent epidermal areas, where the infection is transmitted to the
277 basal keratinocytes. As basal keratinocytes differentiate vertically to the suprabasal layers
278 and their nectin-4 expression increases, the virus spreads laterally and the infected
279 keratinocytes subsequently form syncytia. Infection of dermal endothelial cells was very rare,
280 but not completely absent. We speculate that the infection is subsequently cleared around
281 13 dpi by infiltrating MV-specific T cells, which first migrate into the dermis and later into the
282 epidermis.
283

284 **Discussion**

The pathogenesis of MV skin infection and subsequent skin rash is not well understood. Here, we aimed to identify the cell types involved in MV infection of skin, and the kinetics of viral dissemination in relation to onset of rash. Based on observations from experimentally infected NHPs, *ex vivo* infected human skin explants and *in vitro* infected primary keratinocytes, we initially observed MV-infected perivascular, perifollicular and periadnexal dermal immune cells, followed by dissemination to epidermal keratinocytes. Skin infection preceded onset of rash by 3 to 4 days.

The dermis contains several potential target cells for MV infection. Due to the blood vessels and capillaries that run through it, the dermis is filled with $CD150^+$ lymphoid and myeloid cells that traffic through or reside in the tissue. $CD4^+$ and $CD8^+$ T cells localise and move differently in the skin [31]. Slow-moving $CD8^+$ resident memory T cells (T_{RM}) reside in the epidermis and hair follicles, while highly motile $CD4^+$ effector memory T cells (T_{EM}) migrate into the dermis and recirculate systemically [32]. We detected MV-infected T cells in the dermis from 9 dpi onward, but never in the epidermis at that time point. Previous studies have shown that $CD4^+$ T_{EM} cells are highly susceptible to MV infection [26, 33]. Interaction of MV-infected T cells with skin-resident APCs may result in further cutaneous spread. T cells have been described in human skin to cluster with APCs around appendages, such as hair follicles [34-36]. We did not observe such T cell clusters in NHPs, most likely due to T cell depletion that occurs systemically and peaks around 9 dpi [26]. Whether this depletion leads to the loss of pre-existing skin-resident memory T cells remains to be studied. Additionally, we and others have observed MV-infected T cells and APCs around hair follicles and sebaceous glands [15, 37], which are surrounded by nectin-4^+ epithelial cells [25]. The close proximity of these infected

cells to the basal keratinocytes may lead to the spread of MV infection from the dermis to epidermis.

The epidermis consists predominantly of keratinocytes, which express nectin-4 and are susceptible to MV infection [24]. We were not able to determine the expression of nectin-4 in the NHP epidermis due to the lack of cross-reactive antibodies. However, in accordance with the previous study, we show primary human keratinocytes express nectin-4 and its expression is upregulated upon differentiation [25]. We show here that nectin-4 expression plays a role in the susceptibility of keratinocytes to *in vitro* MV infection: higher expression of nectin-4 resulted in higher susceptibility. This led to the question whether the keratinocytes of an EDSS patient, which have strongly reduced expression of nectin-4, were susceptible to MV infection. We found that, despite its very low expression, the nectin-4 mutant could still facilitate MV infection *in vitro*. Residual nectin-4 activity in this EDSS patient therefore still allows binding of MV haemagglutinin protein and hence facilitates viral entry. Notably, the missense mutation p.Thr185Met is located in the second immunoglobulin-like domain, while MV-binding interfaces of nectin-4 are located in three loops of its most external domain.

Another cell type of interest in the epidermis is the LC, a subset of DCs. Although we could not observe MV-infected LCs in our human skin *ex vivo* model, LCs are known to be susceptible to MV infection [38-40]. The activation status of the cells also determines their susceptibility, since immature LCs are not susceptible to MV infection, while mature ones are [28]. This offers an explanation to why the LCs were not susceptible to MV infection in our *ex vivo* model: the cells might still have been in their immature state. We were also not able to identify LCs in cynomolgus macaque skin tissues due to the unavailability of cross-reactive

antibodies. The susceptibility of LCs to MV infection *in vivo* and their role in the pathogenesis of measles skin rash remain to be determined. Additionally, LCs express Langerin that can act as an attachment, but not entry, receptor to MV [28] and thus can indirectly introduce MV infection to the epidermal keratinocytes by acting as an attachment hub for the virus from the dermis. Although we were able to clearly identify APCs and T cells in the dermis, we were not able to find HLA-DR$^+$ or CD3$^+$ cells in the epidermis. The involvement of these cells in the pathogenesis of MV infection in the epidermis remains to be elicited.

DCs and macrophages occupy the dermis as professional APCs and phagocytes, respectively. Macrophages are present in high numbers and are associated with blood or lymphatic vessels, while dermal DCs have been found to form clusters with T cells, suggesting the presence of an inducible structure of macrophages, DCs and T cells that may function as a skin-associated lymphoid tissue [41, 42]. In the respiratory tract, DCs and macrophages act as Trojan horses during MV infection by spreading the virus to the lymphocytes in draining lymph nodes [7, 43-46]. Migrating or patrolling MV-infected DCs and macrophages may play the same role in the skin as they do in the respiratory tract. However, these cells may also play a crucial role as innate immune cells that inhibit infection. Close communication of MV-infected DCs and macrophages with T cells can lead to activation of MV-specific immune responses and subsequently to the development of rash. The role of these immune responses in the development of rash has been highlighted in immunocompromised patients with MV infection that do not develop skin rash [14].

Blood vessels and capillaries run through the dermis. The capillaries penetrate into the dermal papillae, from where the distance to the epidermis is minimal, and the distribution of the

356 capillary loops differs according to the type of the skin. The capillary bed consists of an
357 arteriole, which gives rise to metarterioles and subsequently hundreds of capillaries. The
358 capillaries provide the dermis and epidermis with nutrition and oxygen, and connect to
359 venous capillarioles and further to a venule. Inflammation due to infection may cause
360 prolonged vasodilatation and increased capillary permeability. This hyperaemic reaction
361 allows the release of chemokines by skin-resident cells, such as memory immune cells and
362 keratinocytes, that leads to the infiltration of various immune cells, such as macrophages and
363 lymphocytes. The vasodilatation also causes erythema and oedema [47]. Given that measles
364 rash is described as maculopapular (*i.e.* small with raised bumps) and erythematous (*i.e.* red),
365 and oedema can be observed in MV-infected skin [15], we speculate that hyperaemia is
366 responsible for the appearance of the erythematous maculopapular rash. Although
367 theoretically it is possible to investigate the presence of hyperaemia in our *in vivo* model by
368 showing an increased number of erythrocytes in the cutaneous blood vessels, we could not
369 perform the calculation fairly, since the animals were sacrificed by exsanguination.
370
371 MV infection in the skin gives a unique appearance of rash compared to other viral
372 exanthemata. Rubella rash, for example, has been described as macroscopically similar to
373 measles rash, since it gives a pink-reddish “rubelliform” maculopapular rash. However, in
374 rubella, viral infection takes place deeper in the dermis, in contrast to measles skin infection
375 that occurs more superficially in the dermis. Infection of the keratinocytes, which is typical
376 for measles rash, does not occur during rubella virus infection [48]. In contrast, varicella zoster
377 virus (VZV), as a representative of the *Herpesviridae* family member, has similar target cells
378 in the dermis and epidermis as MV, but displays a different type of rash. VZV infects
379 perivascular macrophages and DCs as well as keratinocytes, but the infection leads to the

appearance of spots that turn into itchy blisters [49]. Arboviral exanthemata, on the other hand, have a different route of infection, but often present overlapping outcomes in the skin. Dengue virus is introduced into the body through a mosquito bite and injected into the bloodstream, with spillover to the epidermis and the dermis. This spillover causes infection of LCs and keratinocytes. Dengue virus spreads systemically through the infection of monocytes and macrophages. The virus also causes vascular leakage through infection of endothelial cells, leading to the appearance of minor haemorrhagic lesions [50]. Although petechial rash is one of the clinical manifestations of dengue virus infection, morbilliform rash is also often described during classical dengue fever [51]. Altogether, these findings, including ours, strongly suggest that the appearance of rash, especially during measles, is closely linked to the viral tropism, the availability and location of susceptible target cells and the subsequent immune responses to clear the infection.

MV infects the respiratory epithelial cells and is shed apically into the mucus lining the lumen of the upper and lower respiratory tract, which is void of CD150 or nectin-4. The virus is thus transported to the throat by the mucociliary escalator and expelled into the air by coughing [52]. The role of MV skin infection in viral transmission is still a subject of speculation. The outer layer of the epidermis consists of dead keratinised cells. Whether these dead cells allow the attachment of MV and hence the release of dead-cell-associated virus particles into the air remains to be investigated [15].

In conclusion, our study offers a new explanation to the pathogenesis of measles skin rash: MV-infected lymphocytes and myeloid cells enter the dermis, where the infection spreads to the susceptible cells in the vicinity of dermal papillae, hair follicles, sebaceous glands and

404 blood vessels in the superficial dermis. The infection spreads laterally and apically to the
405 epidermis in a nectin-4-dependent manner. The infection is cleared several days later by
406 infiltrating MV-specific T cells, accompanied by the appearance of oedema and hyperaemia
407 that give the appearance of an erythematous morbilliform rash.

Materials and Methods

Ethical statement

All NHP samples were derived from previously published studies, and no new experimental infections were performed [26]. Studies involving the use of primary keratinocytes were approved by the local ethics committee, and written informed consent was obtained from both the EDSS1 patient and the healthy volunteers [25]. Studies using human skin tissue were performed in accordance with the Amsterdam University Medical Centres (AUMC) institutional guidelines with approval of the Medical Ethics Review Committee of the AUMC, location Academic Medical Centre, Amsterdam, the Netherlands, reference number: W15_089 # 15.0103. All samples were handled anonymously.

Cells

Culture of normal and EDSS primary human keratinocytes was carried out as previously described [25]. Keratinocytes were cultured till sub-confluence in serum-free Keratinocyte Growth Medium (KGM, Invitrogen) containing 0.15 mM Ca^{2+} (proliferating keratinocytes), and then induced to differentiate by culturing for further 3 days in a 3:1 mixture of DMEM and Ham's F12 media (Invitrogen, Palo Alto, CA) containing FCS (10%), insulin (5 µg/ml), transferrin (5 µg/ml), adenine (0.18 mM), hydrocortisone (0.4 µg/ml), cholera toxin (0.1 nM), triiodothyronine (2 nM), EGF (10 ng/ml), glutamine (4 mM), and penicillin-streptomycin (50 IU/ml) (differentiated keratinocytes). Epstein-Barr virus- (EBV-) transformed B-lymphoblastoma cell line (BLCL) and human broncho-alveolar carcinoma (NCI-H358) cell lines were grown in RPMI-1640 medium supplemented with 10% of fetal bovine serum (FBS), 100 IU of penicillin/ml, 100 µg of streptomycin/ml and 2 mM glutamine (R10F medium). Vero cells expressing human CD150 (Vero-CD150) were grown in Dulbecco's modified Eagle medium

(DMEM) supplemented with 10% of FBS, 100 IU of penicillin/ml, 100 µg of streptomycin/ml and 2 mM glutamine (D10F medium) [53]. Human embryonic kidney (HEK) 293T cells were grown in D10F medium supplemented with 1 mM sodium pyruvate and non-essentials amino acids. All cells were cultured in a humidified incubator at 37° C with 5% of CO_2.

Tissues

Residual skin materials were obtained from six different adult human donors undergoing correctional surgery and stored at 4° C overnight. The skin was shaved using a dermatome (0.3 mm, Zimmer Biomet, UK). For the preparation of full skin sheets, which consist of dermis and epidermis, the shaved skin was cut into circular sheets (diameter approximately 1 cm) using a skin biopsy punch and cultured in IMDM supplemented with 10% of FCS, 100 IU of penicillin/ml, 100 µg of streptomycin/ml (Invitrogen), 2 mM glutamine and 20 µg/ml gentamicine (Centrafarm, Netherlands) (I10F medium), with the epidermis facing upward. The full skin pieces were stored in a 24-well plate in I10F medium. For the preparation of epidermal sheets, shaved skin was incubated in I10F medium in the presence of 1 U/ml of dispase (Roche Diagnostics) for 1 h at 37° C or 0.5 U/ml overnight at 4° C. The epidermis was separated from dermis using a pair of forceps and cut into circular sheets using a skin biopsy punch. The epidermal or dermal sheets were stored in a 24-well plate in I10F medium, with the keratin layer of the epidermis facing upward.

Viruses

All recombinant MV strains used in this study were described previously: recombinant MV strain Khartoum-Sudan (KS) expressing the fluorescent protein Venus from an additional transcription unit in position 1 or 3 (rMV^{KS}Venus(1) or (3)) [54] and strain IC323 expressing

456 the fluorescent protein EGFP in position 1 (rMV^{IC323}EGFP(1)) of the viral genome [29] were
457 based on wild type viruses. An rMV^{KS} expressing EGFP in position 3 of the viral genome
458 engineered to be unable to recognise nectin-4 (referred to as the 'nectin-4-blind (N4b)' rMV$^{KS\text{-}N4b}$EGFP(3)) was also included in this study [55]. Virus titres were determined by endpoint
460 titration on Vero-CD150 cells, and were expressed as 50% tissue culture infectious dose
461 ($TCID_{50}$) per ml calculated as described by Reed and Muench [30].
462
463 **Sequencing**
464 Partial sequences of plasmid 3XFLAG containing wild-type or mutant nectin-4 (p. Thr185Met)
465 insert were obtained with Applied Biosystems 3130xl Genetic Analyser, according to the
466 instructions provided by the manufacturer. The primers used in this assay were: 5'- CCT-GCC-
467 CTC-ACT-GAA-TCC-TG-3' and 5'-ACA-CCC-ACC-ACC-ACC-ACC-GA-3'. The obtained sequences
468 were analysed with BioEdit software.
469
470 **Transfection**
471 De Wit *et al.* have previously described transfection of HEK 293T cells [56]. In brief, prior to
472 transfection, HEK 293T cells (3×10^6) were seeded into gelatinised 10-cm^2 culture dishes. The
473 cells were transiently transfected overnight in the present of $CaCl_2$ with 3XFLAG plasmid (30
474 µg) containing wild-type or mutant nectin-4 insert. After 6 h of transfection, the cells were
475 treated with trypsin and seeded into gelatinised 24-well plates. After 36 h of transfection, the
476 cells were treated with trypsin and the nectin-4 expression levels were assessed with flow
477 cytometry.
478
479 ***In vitro* MV infection**

Adherent primary keratinocytes were either inoculated directly or were treated with trypsin-EDTA (0.05%) and inoculated in suspension with the three different rMV strains at an MOI of 1. After 2 h, the suspension cells were washed to remove unbound virus and seeded onto 24-well plates in K medium. After 48 h of infection, the cells were observed under an inverted-laser scanning LSM-700 microscope (Zeiss) and the infection percentages were assessed by flow cytometry. Transiently transfected HEK 293T cells were inoculated directly with rMV^{KS}Venus(3) at an MOI of 3. After 24 h of infection, the infection percentages were measured by flow cytometry.

Ex vivo MV infection

Full skin pieces, dermal or epidermal sheets were inoculated with cell-free rMV^{KS}Venus(3). Briefly, 200 µl of pure virus stock (3.7×10^6 $TCID_{50}$/ml) was added to each well of a 24-well plate, and the skin sheets were added on top of the liquid with the epidermis facing upwards. While full skin and epidermal sheets remained afloat, dermal sheets tended to sink and both apical and basolateral surfaces were exposed to virus. After 2 h at 37°C, I10F medium was added to the wells. The progression of infection was observed at 2, 4 and 7 dpi under the inverted laser scanning microscope. Full skin pieces, dermal or epidermal sheets were fixed in 4% paraformaldehyde (PFA) for at least 24 h and subsequently stored in PBS or as formalin-fixed paraffin-embedded tissue blocks.

Measurement of MV production by infected keratinocytes

Supernatant of MV-infected keratinocytes was titrated into 96-well plates containing Vero-CD150 cells (1×10^4 cells/well). The titre of the virus was expressed as $TCID_{50}$/ml and calculated as described above.

504

505 **Flow cytometry**

506 Flow cytometry was performed using a BD FACSCanto II. Primary keratinocytes or HEK 293T
507 cells were labelled with nectin-4^{PE} antibody (clone 337516; R&D Systems) to assess the
508 expression of nectin-4. Isotype control (Isotype^{PE}, clone 27-35, BD Biosciences) antibody was
509 included to assess the level of background staining. NCI-H358 cells and BLCL were included as
510 positive and negative controls for nectin-4 expression, respectively. All cells were fixed with
511 2% of PFA prior to measurement of the percentage of cells expressing the virus-encoded
512 fluorescent protein. Mock-infected cells were included as infection control. Supernatants
513 from full skin pieces (n = 3 donors), dermal (n = 1 donor) or epidermal sheets (n = 3 donors)
514 were isolated at 2, 4 and 7 dpi and emigrant cells were isolated after undergoing
515 centrifugation. Antibodies used in this experiment is listed in Table 1. Data was acquired with
516 BD FACSDiva software and analysed with FlowJo software.

517

518 **Table 1.** List of antibodies used in flow cytometry to identify the phenotypes of cells in full
519 skin, dermal and epidermal sheets.

Antigen	Clone	Fluorochrome
CD4	SK3	PerCP
CD19	J3-119	PE-Cy7
CD3	UCHT1	APC
HLA-DR	L243	Pacific Blue
CD8	SK1	AmCyan

520

521 ***In situ* analyses**

Immunohistochemistry was performed using monoclonal antibodies directed to MV N protein (clone 83KKII, Chemicon [57]) or rabbit polyclonal antibody directed to GFP (Invitrogen). Goat anti-mouse IgG1 or goat anti-rabbit antibody conjugated with biotin was included as secondary antibody. Streptavidin-horseradish peroxidase was added for signal detection. Dual-IF assays were performed using mouse monoclonal antibodies directed to CD45 (clone 2B11+PD7/26; DAKO), CD3 (clone F7.2.38; DAKO), CD31 (clone JC70A; DAKO), cytokeratin (clone AE1/AE3; DAKO), S100A8/A9 complex (clone MAC387; Abcam), or HLA-DR (clone L243; BioLegend) in combination with rabbit polyclonal antibody directed to GFP. Goat anti-rabbit-IgG-Alexa Fluor (AF)488 (Invitrogen) and goat anti-mouse IgG-AF594 (Invitrogen) were included as secondary antibodies. Formalin-fixed, paraffin-embedded tissues were sectioned at 3 µm, deparaffinised and rehydrated prior to antigen retrieval. Antigen retrieval for MV N protein staining was performed in the presence of 0.1% protease in pre-warmed phosphate buffered saline (PBS) for 10 minutes at 37° C. Antigen retrieval for other stainings was performed in citrate buffer (10 mM, pH = 6.0) with heat induction. Sections were incubated with primary antibody overnight at 4° C before incubation with secondary and tertiary antibodies. For IF assays, the slides were mounted with ProLong Diamond Antifade Mountant with DAPI (Thermo Fisher Scientific) prior to fluorescence detection with the inverted laser scanning microscope.

Funding

BMN and TBHG were supported by Aidsfonds (P-11118), European Research Council, Advanced grant (670424). BML is supported by the Indonesian Endowment Fund for Education (grant no. 20150822023688). The funders had no role in study design, data collection and analysis, decision to publish, or preparation of the manuscript.

546

547 **Acknowledgment**

548 We are grateful to the Boerhaave Medical Centre (Amsterdam, the Netherlands) and A.

549 Knottenbelt (Flevo Clinic Almere, the Netherlands) for the provision of human skin tissues,

550 Peter R. W. A. van Run and Daryl Geers for the excellent technical assistance.

551

552 **Reference list**

553 1. Rota PA, Moss WJ, Takeda M, de Swart RL, Thompson KM, Goodson JL. Measles. Nat
554 Rev Dis Primers. 2016;2:16049. doi: 10.1038/nrdp.2016.49. PubMed PMID: 27411684.
555 2. Tatsuo H, Ono N, Tanaka K, Yanagi Y. SLAM (CDw150) is a cellular receptor for measles
556 virus. Nature. 2000;406(6798):893-7. doi: 10.1038/35022579. PubMed PMID: 10972291.
557 3. Muhlebach MD, Mateo M, Sinn PL, Prufer S, Uhlig KM, Leonard VH, et al. Adherens
558 junction protein nectin-4 is the epithelial receptor for measles virus. Nature.
559 2011;480(7378):530-3. doi: 10.1038/nature10639. PubMed PMID: 22048310.
560 4. Noyce RS, Richardson CD. Nectin 4 is the epithelial cell receptor for measles virus.
561 Trends Microbiol. 2012;20(9):429-39. doi: 10.1016/j.tim.2012.05.006. PubMed PMID:
562 22721863.
563 5. Mateo M, Generous A, Sinn PL, Cattaneo R. Connections matter--how viruses use cell-
564 cell adhesion components. J Cell Sci. 2015;128(3):431-9. doi: 10.1242/jcs.159400. PubMed
565 PMID: 26046138.
566 6. Cifuentes-Munoz N, Dutch RE, Cattaneo R. Direct cell-to-cell transmission of
567 respiratory viruses: The fast lanes. PLoS Pathog. 2018;14(6):e1007015. doi:
568 10.1371/journal.ppat.1007015. PubMed PMID: 29953542.
569 7. Lemon K, de Vries RD, Mesman AW, McQuaid S, van Amerongen G, Yuksel S, et al.
570 Early target cells of measles virus after aerosol infection of non-human primates. PLoS Pathog.
571 2011;7(1):e1001263. doi: 10.1371/journal.ppat.1001263. PubMed PMID: 21304593.
572 8. de Swart RL, Ludlow M, de Witte L, Yanagi Y, van Amerongen G, McQuaid S, et al.
573 Predominant infection of CD150+ lymphocytes and dendritic cells during measles virus
574 infection of macaques. PLoS Pathog. 2007;3(11):e178. doi: 10.1371/journal.ppat.0030178.
575 PubMed PMID: 18020706.

576 9. Laksono BM, de Vries RD, Verburgh RJ, Visser EG, de Jong A, Fraaij PLA, et al. Studies
577 into the mechanism of measles-associated immune suppression during a measles outbreak in
578 the Netherlands. Nat Commun. 2018;9(1):4944. doi: 10.1038/s41467-018-07515-0. PubMed
579 PMID: 30470742.
580 10. Ludlow M, Lemon K, de Vries RD, McQuaid S, Millar EL, van Amerongen G, et al.
581 Measles virus infection of epithelial cells in the macaque upper respiratory tract is mediated
582 by subepithelial immune cells. J Virol. 2013;87(7):4033-42. doi: 10.1128/jvi.03258-12.
583 PubMed PMID: 23365435.
584 11. Sawatsky B, Cattaneo R, von Messling V. Canine Distemper Virus Spread and
585 Transmission to Naive Ferrets: Selective Pressure on SLAM-Dependent Entry. J Virol.
586 2018;92(15):e00669-18. doi: JVI.00669-18 [pii]
587 10.1128/JVI.00669-18. PubMed PMID: 29793948.
588 12. Racaniello V. Virology. An exit strategy for measles virus. Science.
589 2011;334(6063):1650-1. doi: 10.1126/science.1217378. PubMed PMID: 22194562.
590 13. Rota PA, Moss WJ, Takeda M, de Swart RL, Thompson KM, Goodson JL. Measles. Nat
591 Rev Dis Primers. 2016;2(1):16049. doi: 10.1038/nrdp.2016.49. PubMed PMID: 27411684.
592 14. de Swart RL, Wertheim-van Dillen PM, van Binnendijk RS, Muller CP, Frenkel J,
593 Osterhaus AD. Measles in a Dutch hospital introduced by an immuno-compromised infant
594 from Indonesia infected with a new virus genotype. Lancet. 2000;355(9199):201-2. PubMed
595 PMID: 10675124.
596 15. Liersch J, Omaj R, Schaller J. Histopathological and Immunohistochemical
597 Characteristics of Measles Exanthema: A Study of a Series of 13 Adult Cases and Review of
598 the Literature. Am J Dermatopathol. 2019. doi: 10.1097/DAD.0000000000001431. PubMed
599 PMID: 31021834.

600 16. Magdaleno-Tapial J, Valenzuela-Onate C, Giacaman-von der Weth M, Ferrer-Guillen
601 B, Garcia-Legaz Martinez M, Martinez-Domenech A, et al. Follicle and Sebaceous Gland
602 Multinucleated Cells in Measles. Am J Dermatopathol. 2019;41(4):289-92. doi:
603 10.1097/DAD.0000000000001278. PubMed PMID: 30252698.
604 17. Kimura A, Tosaka K, Nakao T. An immunofluorescent and electron microscopic study
605 of measles skin eruptions. Tohoku J Exp Med. 1975;117(3):245-56. PubMed PMID: 1105894.
606 18. Andres O, Obojes K, Kim KS, ter Meulen V, Schneider-Schaulies J. CD46- and CD150-
607 independent endothelial cell infection with wild-type measles viruses. J Gen Virol. 2003;84(Pt
608 5):1189-97. doi: 10.1099/vir.0.18877-0. PubMed PMID: 12692284.
609 19. Reymond N, Fabre S, Lecocq E, Adelaide J, Dubreuil P, Lopez M. Nectin4/PRR4, a new
610 afadin-associated member of the nectin family that trans-interacts with nectin1/PRR1
611 through V domain interaction. J Biol Chem. 2001;276(46):43205-15. doi:
612 10.1074/jbc.M103810200. PubMed PMID: 11544254.
613 20. Nomura T, Kabashima K, Miyachi Y. The panoply of alphabetaT cells in the skin. J
614 Dermatol Sci. 2014;76(1):3-9. doi: S0923-1811(14)00183-2 [pii]
615 10.1016/j.jdermsci.2014.07.010. PubMed PMID: 25190363.
616 21. Adachi T, Kobayashi T, Sugihara E, Yamada T, Ikuta K, Pittaluga S, et al. Hair follicle-
617 derived IL-7 and IL-15 mediate skin-resident memory T cell homeostasis and lymphoma. Nat
618 Med. 2015;21(11):1272-9. doi: 10.1038/nm.3962. PubMed PMID: 26479922.
619 22. Watanabe R, Gehad A, Yang C, Scott LL, Teague JE, Schlapbach C, et al. Human skin is
620 protected by four functionally and phenotypically discrete populations of resident and
621 recirculating memory T cells. Sci Transl Med. 2015;7(279):279ra39. doi: 7/279/279ra39 [pii]
622 10.1126/scitranslmed.3010302. PubMed PMID: 25787765.

623 23. Romani N, Holzmann S, Tripp CH, Koch F, Stoitzner P. Langerhans cells - dendritic cells
624 of the epidermis. APMIS. 2003;111(7-8):725-40. doi: DOI 10.1034/j.1600-
625 0463.2003.11107805.x. PubMed PMID: 12974775.
626 24. Gourru-Lesimple G, Mathieu C, Thevenet T, Guillaume-Vasselin V, Jegou JF, Boer CG,
627 et al. Measles virus infection of human keratinocytes: Possible link between measles and
628 atopic dermatitis. J Dermatol Sci. 2017;86(2):97-105. doi: 10.1016/j.jdermsci.2017.01.015.
629 PubMed PMID: 28233587.
630 25. Brancati F, Fortugno P, Bottillo I, Lopez M, Josselin E, Boudghene-Stambouli O, et al.
631 Mutations in PVRL4, encoding cell adhesion molecule nectin-4, cause ectodermal dysplasia-
632 syndactyly syndrome. Am J Hum Genet. 2010;87(2):265-73. doi: 10.1016/j.ajhg.2010.07.003.
633 PubMed PMID: 20691405.
634 26. de Vries RD, McQuaid S, van Amerongen G, Yuksel S, Verburgh RJ, Osterhaus AD, et al.
635 Measles immune suppression: lessons from the macaque model. PLoS Pathog.
636 2012;8(8):e1002885. doi: 10.1371/journal.ppat.1002885. PubMed PMID: 22952446.
637 27. de Vries RD, Lemon K, Ludlow M, McQuaid S, Yuksel S, van Amerongen G, et al. *In vivo*
638 tropism of attenuated and pathogenic measles virus expressing green fluorescent protein in
639 macaques. J Virol. 2010;84(9):4714-24. doi: 10.1128/JVI.02633-09. PubMed PMID: 20181691.
640 28. van der Vlist M, de Witte L, de Vries RD, Litjens M, de Jong MA, Fluitsma D, et al.
641 Human Langerhans cells capture measles virus through Langerin and present viral antigens to
642 CD4(+) T cells but are incapable of cross-presentation. Eur J Immunol. 2011;41(9):2619-31.
643 doi: 10.1002/eji.201041305. PubMed PMID: 21739428.
644 29. Hashimoto K, Ono N, Tatsuo H, Minagawa H, Takeda M, Takeuchi K, et al. SLAM
645 (CD150)-independent measles virus entry as revealed by recombinant virus expressing green
646 fluorescent protein. J Virol. 2002;76(13):6743-9. PubMed PMID: 12050387.

647 30. Reed LJ, Muench H. A simple method of estimating fifty percent end points. The
648 American Journal of Hygiene. 1938;27(3):493-7.
649 31. Gebhardt T, Whitney PG, Zaid A, Mackay LK, Brooks AG, Heath WR, et al. Different
650 patterns of peripheral migration by memory CD4+ and CD8+ T cells. Nature.
651 2011;477(7363):216-9. doi: 10.1038/nature10339. PubMed PMID: 21841802.
652 32. Mueller SN, Gebhardt T, Carbone FR, Heath WR. Memory T cell subsets, migration
653 patterns, and tissue residence. Annu Rev Immunol. 2013;31:137-61. doi: 10.1146/annurev-
654 immunol-032712-095954. PubMed PMID: 23215646.
655 33. Laksono BM, Grosserichter-Wagener C, de Vries RD, Langeveld SAG, Brem MD, van
656 Dongen JJM, et al. In Vitro Measles Virus Infection of Human Lymphocyte Subsets
657 Demonstrates High Susceptibility and Permissiveness of both Naive and Memory B Cells. J
658 Virol. 2018;92(8). doi: 10.1128/jvi.00131-18. PubMed PMID: 29437964.
659 34. Bos JD, Zonneveld I, Das PK, Krieg SR, van der Loos CM, Kapsenberg ML. The skin
660 immune system (SIS): distribution and immunophenotype of lymphocyte subpopulations in
661 normal human skin. J Invest Dermatol. 1987;88(5):569-73. doi: 10.1111/1523-
662 1747.ep12470172. PubMed PMID: 3494791.
663 35. Clark RA, Chong B, Mirchandani N, Brinster NK, Yamanaka K, Dowgiert RK, et al. The
664 vast majority of CLA+ T cells are resident in normal skin. J Immunol. 2006;176(7):4431-9. doi:
665 10.4049/jimmunol.176.7.4431. PubMed PMID: 16547281.
666 36. Collins N, Jiang X, Zaid A, Macleod BL, Li J, Park CO, et al. Skin CD4(+) memory T cells
667 exhibit combined cluster-mediated retention and equilibration with the circulation. Nat
668 Commun. 2016;7:11514. doi: 10.1038/ncomms11514. PubMed PMID: 27160938.

669 37. Tirado M, Adamzik K, Boer-Auer A. Follicular necrotic keratinocytes - a helpful clue to
670 the diagnosis of measles. J Cutan Pathol. 2015;42(9):632-8. doi: 10.1111/cup.12529. PubMed
671 PMID: 25965994.
672 38. Steineur MP, Grosjean I, Bella C, Kaiserlian D. Langerhans cells are susceptible to
673 measles virus infection and actively suppress T cell proliferation. Eur J Dermatol.
674 1998;8(6):413-20. PubMed PMID: 9729058.
675 39. Watari E, Shimizu M, Takahashi H. Langerhans cells stimulated by mechanical stress
676 are susceptible to measles virus infection. Intervirology. 2005;48(2-3):145-52. doi:
677 10.1159/000081742. PubMed PMID: 15812188.
678 40. van der Vlist M, de Witte L, de Vries RD, Litjens M, de Jong MA, Fluitsma D, et al.
679 Human Langerhans cells capture measles virus through Langerin and present viral antigens to
680 CD4+ T cells but are incapable of cross-presentation. Eur J Immunol. 2011;41(9):2619-31. doi:
681 10.1002/eji.201041305. PubMed PMID: 21739428.
682 41. Ono S, Kabashima K. Novel insights into the role of immune cells in skin and inducible
683 skin-associated lymphoid tissue (iSALT). Allergo J Int. 2015;24:170-9. doi: 10.1007/s40629-
684 015-0065-1. PubMed PMID: 27069837.
685 42. McLellan AD, Heiser A, Sorg RV, Fearnley DB, Hart DN. Dermal dendritic cells
686 associated with T lymphocytes in normal human skin display an activated phenotype. J Invest
687 Dermatol. 1998;111(5):841-9. doi: 10.1046/j.1523-1747.1998.00375.x. PubMed PMID:
688 9804348.
689 43. de Witte L, Abt M, Schneider-Schaulies S, van Kooyk Y, Geijtenbeek TB. Measles virus
690 targets DC-SIGN to enhance dendritic cell infection. J Virol. 2006;80(7):3477-86. doi:
691 10.1128/JVI.80.7.3477-3486.2006. PubMed PMID: 16537615.

692 44. de Witte L, de Vries RD, van der Vlist M, Yuksel S, Litjens M, de Swart RL, et al. DC-
693 SIGN and CD150 have distinct roles in transmission of measles virus from dendritic cells to T-
694 lymphocytes. PLoS Pathog. 2008;4(4):e1000049. doi: 10.1371/journal.ppat.1000049.
695 PubMed PMID: 18421379.
696 45. Avota E, Gulbins E, Schneider-Schaulies S. DC-SIGN mediated sphingomyelinase-
697 activation and ceramide generation is essential for enhancement of viral uptake in dendritic
698 cells. PLoS Pathog. 2011;7(2):e1001290. doi: 10.1371/journal.ppat.1001290. PubMed PMID:
699 21379338.
700 46. Mesman AW, de Vries RD, McQuaid S, Duprex WP, de Swart RL, Geijtenbeek TB. A
701 prominent role for DC-SIGN+ dendritic cells in initiation and dissemination of measles virus
702 infection in non-human primates. PLoS One. 2012;7(12):e49573. doi:
703 10.1371/journal.pone.0049573. PubMed PMID: 23227146.
704 47. Bliss MR. Hyperaemia. J Tissue Viability. 1998;8(4):4-13. PubMed PMID: 10480965.
705 48. Takahashi H, Umino Y, Sato TA, Kohama T, Ikeda Y, Iijima M, et al. Detection and
706 comparison of viral antigens in measles and rubella rashes. Clin Infect Dis. 1996;22(1):36-9.
707 PubMed PMID: 8824963.
708 49. Ouwendijk WJ, Mahalingam R, de Swart RL, Haagmans BL, van Amerongen G, Getu S,
709 et al. T-Cell tropism of simian varicella virus during primary infection. PLoS Pathog.
710 2013;9(5):e1003368. doi: 10.1371/journal.ppat.1003368. PubMed PMID: 23675304.
711 50. Martina BE, Koraka P, Osterhaus AD. Dengue virus pathogenesis: an integrated view.
712 Clin Microbiol Rev. 2009;22(4):564-81. doi: 10.1128/cmr.00035-09. PubMed PMID: 19822889.
713 51. Korman AM, Alikhan A, Kaffenberger BH. Viral exanthems: An update on laboratory
714 testing of the adult patient. J Am Acad Dermatol. 2017;76(3):538-50. doi:
715 10.1016/j.jaad.2016.08.034. PubMed PMID: 28413059.

716 52. Laksono BM, de Vries RD, McQuaid S, Duprex WP, de Swart RL. Measles Virus Host
717 Invasion and Pathogenesis. Viruses. 2016;8(8). doi: 10.3390/v8080210. PubMed PMID:
718 27483301.
719 53. Ono N, Tatsuo H, Hidaka Y, Aoki T, Minagawa H, Yanagi Y. Measles viruses on throat
720 swabs from measles patients use signaling lymphocytic activation molecule (CDw150) but not
721 CD46 as a cellular receptor. J Virol. 2001;75(9):4399-401. doi: 10.1128/jvi.75.9.4399-
722 4401.2001. PubMed PMID: 11287589.
723 54. Davis ME, Wang MK, Rennick LJ, Full F, Gableske S, Mesman AW, et al. Antagonism of
724 the phosphatase PP1 by the measles virus V protein is required for innate immune escape of
725 MDA5. Cell Host & Microbe. 2014;16(1):19-30. doi: S1931-3128(14)00223-6 [pii]
726 10.1016/j.chom.2014.06.007. PubMed PMID: 25011105.
727 55. Ludlow M, de Vries RD, Lemon K, McQuaid S, Millar E, van Amerongen G, et al.
728 Infection of lymphoid tissues in the macaque upper respiratory tract contributes to the
729 emergence of transmissible measles virus. J Gen Virol. 2013;94(Pt 9):1933-44. doi:
730 10.1099/vir.0.054650-0. PubMed PMID: 23784446.
731 56. de Wit E, Spronken MI, Vervaet G, Rimmelzwaan GF, Osterhaus AD, Fouchier RA. A
732 reverse-genetics system for Influenza A virus using T7 RNA polymerase. J Gen Virol.
733 2007;88(Pt 4):1281-7. doi: 10.1099/vir.0.82452-0. PubMed PMID: 17374773.
734 57. Whistler T, Blackburn N. A rapid culture assay for examining measles virus infections
735 from urine specimens. Clin Diagn Virol. 1997;7(3):193-200. PubMed PMID: 9126689.
736
737

738 **Fig 1. The appearance of MV-infected cells in the skin precedes the appearance of rash.**
739 Macroscopic evaluation of MV infection in two cynomolgus macaques: animal #38 (a – f) and
740 animal #37 ((g – l), table S1 in [26]). (a – c; g – i) Normal light: Rash was prominent at 11 dpi.
741 (d – f; j – l) Fluorescence: MV-infected sites (fluorescence) in the skin preceded the rash at 8
742 dpi and diminished around 13 dpi.
743
744 **Fig 2. Infection of macaque skin starts in the dermis and spreads to the epidermis.**
745 Immunohistochemical staining of MV-infected macaque skin biopsies collected at 9 (a and d),
746 11 (b and e) and 13 (c and f) dpi. (a and d) Most MV N^+ cells could be found in the dermal
747 papillae, although a few single infected cells were detected in the basal layer of the epidermis
748 at 9 dpi. (b and e) At 11 dpi, prominent infection was observed near hair follicle and sebaceous
749 gland (arrow). The infection in the epidermis has progressed further in the suprabasal layers
750 (arrows). (c and f) The infection in the dermis was no longer detected at 13 dpi. The infection
751 in the epidermis had reached the most superficial layers. (g – i) A syncytium (ellipse) in the
752 epidermis of macaque skin collected at 9 dpi stained with haematoxylin and eosin (HE), or
753 with green fluorescence protein (GFP) and MV N antibodies, respectively. Scale bars of (a), (c)
754 and (g – i): 50 µm; Scale bar of (b): 100 µm; Scale bars of (d – f): 20 µm.
755
756 **Fig 3. The phenotypes of MV-infected cells in the dermis and epidermis throughout the**
757 **course of infection.** Serial sections of skin (top to bottom) of three macaques (left to right)
758 euthanised at three different time points (indicated above). The sections were double-stained
759 with antibodies to EGFP (green) and several cell-specific markers (red), as indicated on the
760 left of each row. (a) At 9 dpi, MV-infected $CD45^+$ white blood cells (inset, arrow) could be
761 detected in the superficial dermis. (b) Some of these MV-infected white blood cells were $CD3^+$

762 T cells, which were present in the dermis, mostly in a more basal area, with speckled GFP
763 signal in their cytoplasm (inset, arrow). (c) MV-infected S100A8/A9 complex$^+$ macrophages
764 (inset, arrow) were also found abundantly in the superficial dermis. (d) MV-infected cells in
765 the dermis were often found in or around CD31$^+$ blood vessels (inset). (e) In the epidermis,
766 MV-infected cells were mostly keratinocytes (inset, arrow), although MV-infected non-
767 keratinocyte cells (inset, asterisk) were observed in the basal epidermis. (f) At 11 dpi, MV-
768 infected white blood cells (inset, arrow), which were (g) T cells in the dermal papillae (inset,
769 arrow) were in close proximity to (h) uninfected macrophages (inset) and (i) blood vessels. (j)
770 The infection in keratinocytes had progressed apically and laterally. (k – o) MV-infected cells
771 had mostly disappeared from the dermis at 13 dpi. The dermis and epidermis were filled with
772 white blood cells. Dm: Dermis; Ep: Epidermis. Scale bar: 50 µm.
773
774 **Fig 4. The location of MV-infected cells and the interaction with other cells in their proximity.**
775 (a – f) MV-infected cells in the dermis and (g – l) in the epidermis. (a) MV-infected CD45$^+$ white
776 blood cells (arrow) in the dermis, especially near the basal layer of the epidermis. (b) MV-
777 infected CD3$^+$ T cells, although mostly found in the dermal papillae at 9 and 11 dpi, in reticular
778 dermis at 13 dpi, surrounded by uninfected T cells. (c) MV-infected cell in the dermis
779 interacted with HLA-DR$^+$ APC, forming a long EGFP$^+$ dendrite (arrow). (d) More often, MV-
780 infected cells (arrow) located around or in blood vessels and, (e) rarely, MV-infected
781 endothelial cells (arrow) could be found together with those cells. (f) Spindle- or dendritic-
782 like MV-infected cells were negative for all tested cell markers. (g – i) In the epidermis, MV-
783 infected white blood cells could be found since 11 dpi, either interacting with other white
784 blood cells (g) or other MV-infected epidermal cells (h). (i) White blood cells appeared to
785 infiltrate the MV-infected cells in the epidermis. (j – k) Serial slides of MV-infected epidermis

786 at 13 dpi. MV-infected white blood cells that were negative for cytokeratin marker could be
787 found in the basal layer of the epidermis, presumably Langerhans cells. These cells were in
788 close proximity with infected keratinocytes (k). (l) MV-infected keratinocytes in the absence
789 of other cells. Scale bars of (a – d), (f), (g) and (j – l): 10 µm; Scale bars of (e) and (h – i): 20
790 µm.
791
792 **Fig 5. *Ex vivo* MV infection of human epidermis and dermis sheets.** (a) MV^+ cells (green) were
793 detectable as early as 2 dpi in the epidermis and were present in higher numbers in the dermis
794 than in the epidermis. (b) Percentages of infected cells in each cell subset of lymphocyte and
795 non-lymphocyte populations isolated from epidermis, dermis and full skin at 2, 4 and 7 dpi.
796 APC: antigen-presenting cell. Scale bars: 200 µm.
797
798 **Fig 6. The susceptibility of proliferating and differentiated keratinocytes to *in vitro* MV**
799 **infection.** A higher number of infected keratinocytes (green) was detected in differentiated
800 than in proliferating cultures, regardless of MV strain. All experiments were done in duplicate.
801 NCI-H358: human broncho-alveolar carcinoma cell line; BLCL: EBV-transformed B-
802 lymphoblastoma cell line. HD1 or HD2: primary keratinocyte culture from healthy donor 1 or
803 2; EDSS: primary keratinocyte culture from EDSS patient; KS: rMV^{KS}Venus(3); IC323:
804 rMV^{IC323}EGFP(1); N4B: $rMV^{KS\text{-}N4b}$EGFP(3). Scale bars: 200 µm.
805
806 **Fig 7. Production of cell-free virus by MV-infected proliferating and differentiated**
807 **keratinocytes and susceptibility of HEK 293T cells transiently expressing wild-type or**
808 **mutant nectin-4 to MV infection.** (a) MV-infected proliferating and differentiated
809 keratinocytes of an EDSS patient produced a comparable amount of cell-free virus to that of

the healthy donors. (b) Expression of nectin-4 on HEK 293T cells was measured prior to infection (left graph). Venus fluorescence was detected in these cells after 24 h of infection (right graph). Mock cells were taken as control for transfection and infection. HEK 293T cells were transfected with plasmid containing wild-type or mutant p.Thr185Met insert. All experiments were done in duplicate. HD1 or HD2: primary keratinocyte culture from healthy donor 1 or 2; EDSS: primary keratinocyte culture from EDSS patient; KS: rMV^{KS}Venus(3); IC323: rMV^{IC323}EGFP(1); KS-N4B: rMV$^{KS\text{-}N4b}$EGFP(3); N4-wt: wild-type nectin-4; N4-185: nectin-4-T185M.

Fig 8. Model for pathogenesis of measles skin rash. During viremia, MV-infected T cells and macrophages migrate to the dermis via the capillaries and interact with (a) tissue-resident lymphoid and myeloid cells and epidermal LCs residing near the basal lamina. This interaction leads to the infection of surrounding CD150^{+} tissue-resident immune cells and nectin-4^{+} epithelial cells. Alternatively, MV-infected T cells and macrophages migrate in close proximity to: (b) the hair follicle or (c) the sebaceous gland via the capillary, where they infect an aggregate of tissue-resident T cells and macrophages, and further spread the infection to nearby keratinocytes and LCs. Infection of basal keratinocytes leads to lateral and apical spread of the virus to the superficial layers of the epidermis. Several days later, (d) hyperaemic responses allow the recruitment of MV-specific CD8^{+} cytotoxic T cells and macrophages, resulting in (e) recognition and (f) clearance of the infected cells. Hyperaemia and subsequent oedema are the histological correlates of maculopapular erythematous measles rash.

833 **S1. MV-infected LCs were not observed after *ex vivo* infection of human epidermal sheets.**

834 LCs (magenta) were present in abundance in human epidermal sheets. MV-infected cells

835 (green) appeared at 2 dpi and their number increased by 4 dpi. However, none of these

836 infected cells were LCs. Magenta: CD1a; Green: GFP; Blue: DAPI. Scale bars: 200 µm.

837

838 **S2. Nectin-4 was expressed at a relatively low level in proliferating human primary**

839 **keratinocytes.** The expression level increased during differentiation. The expression of

840 nectin-4 was abrogated in EDSS patient's keratinocytes and differentiation did not result in

841 increased nectin-4 expression. NCI-H358 and BLCL were included as positive and negative

842 controls of nectin-4 expression, respectively.

843

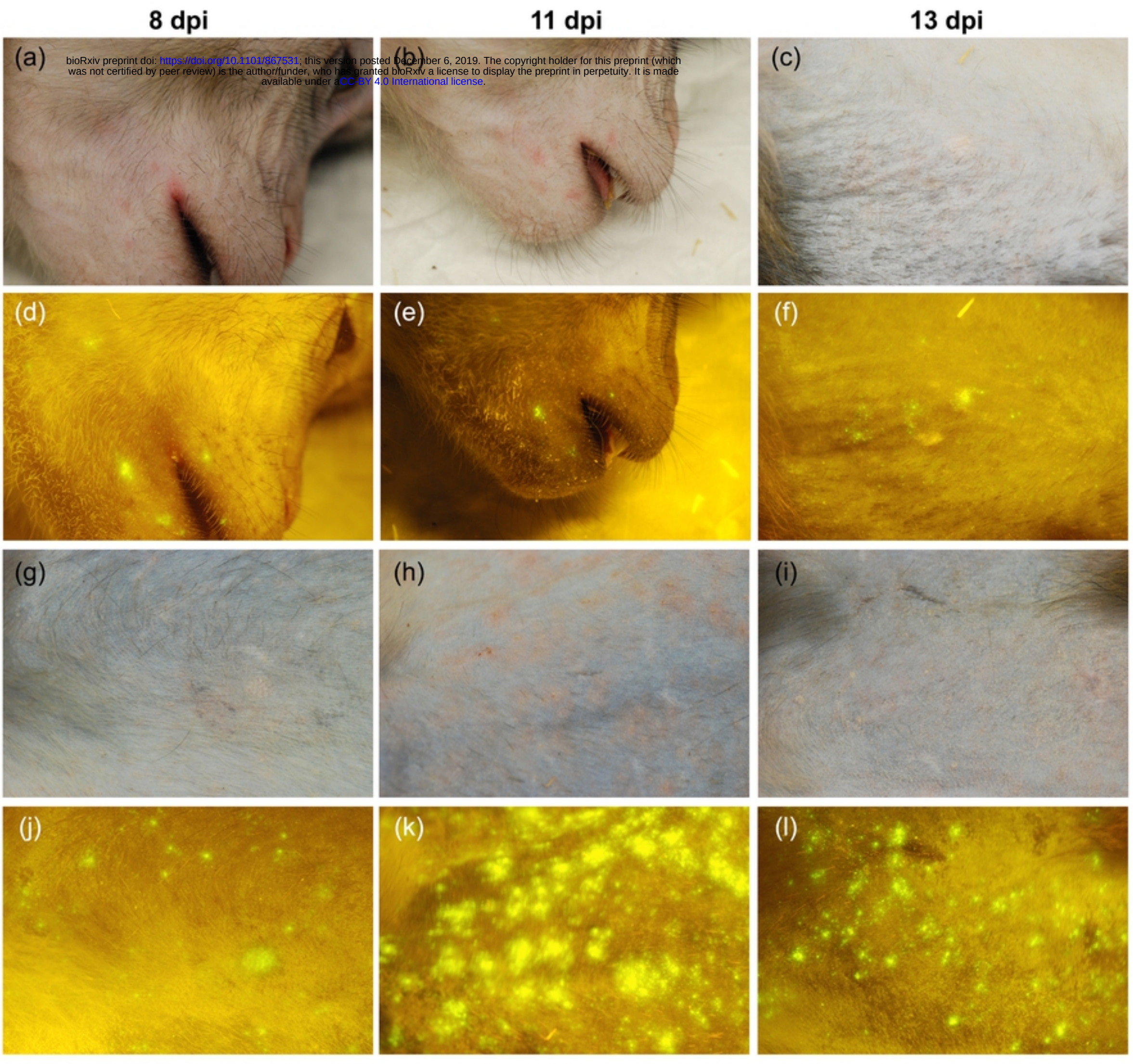

Figure 1

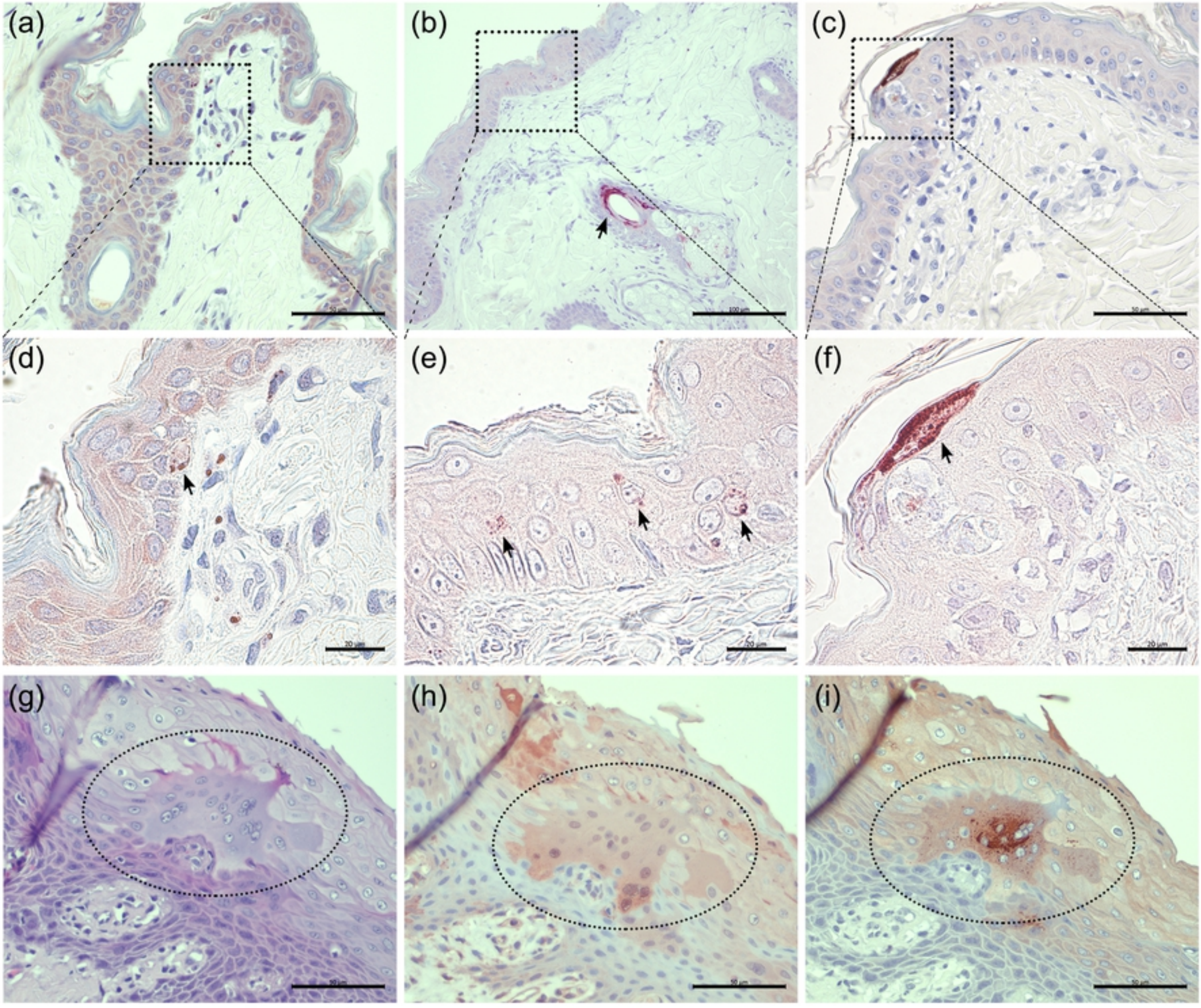

Figure 2

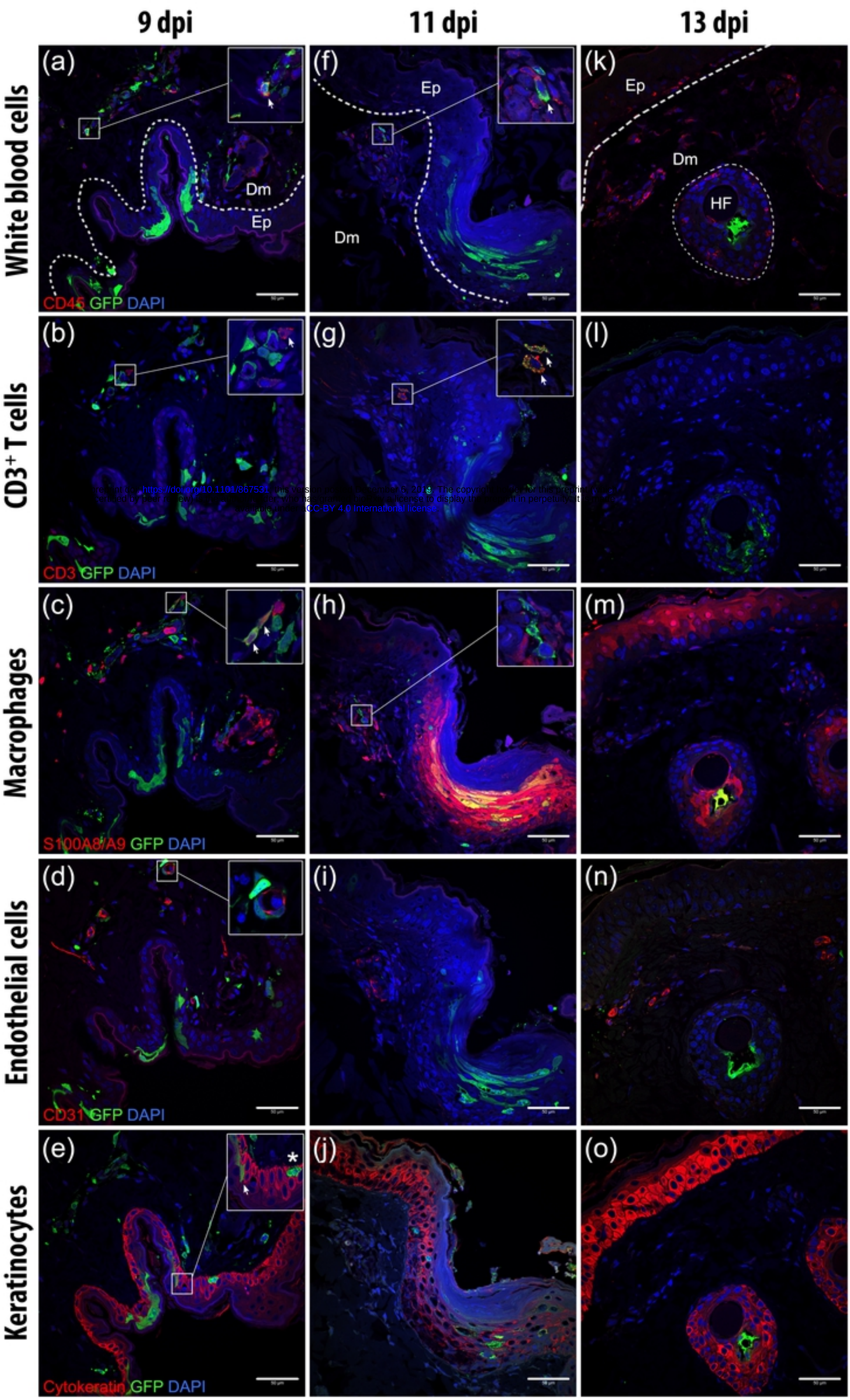

Figure 3

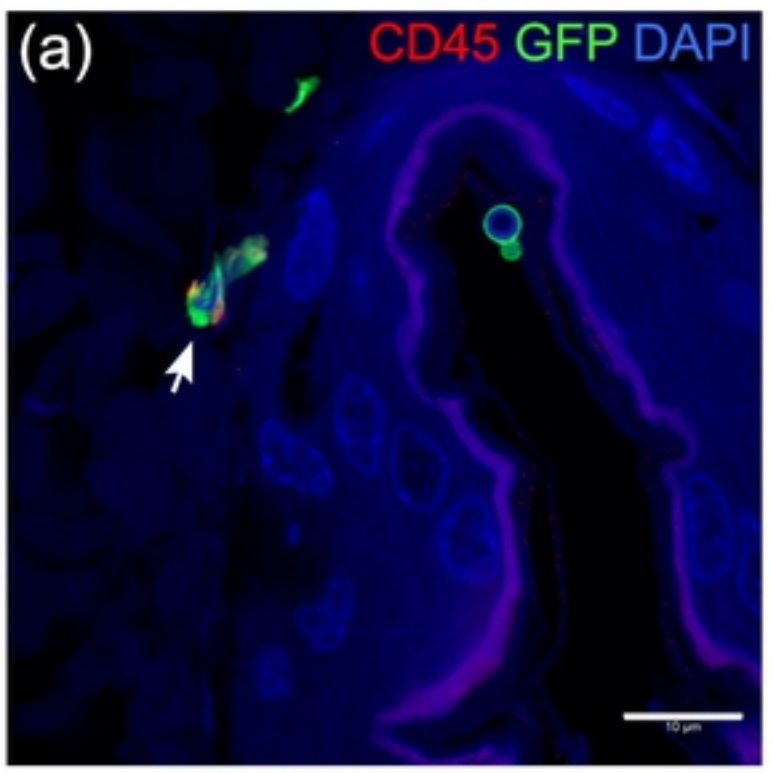

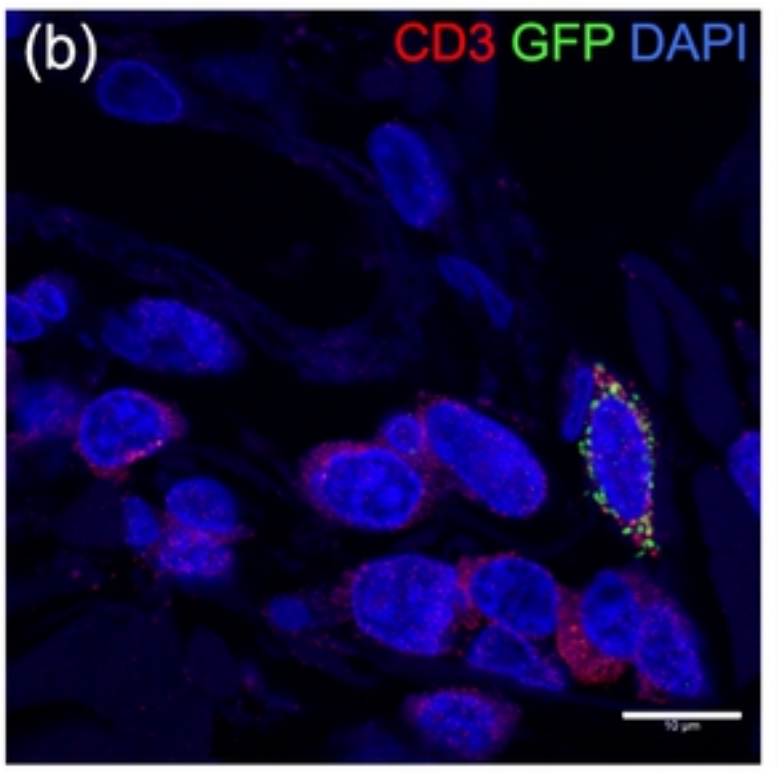

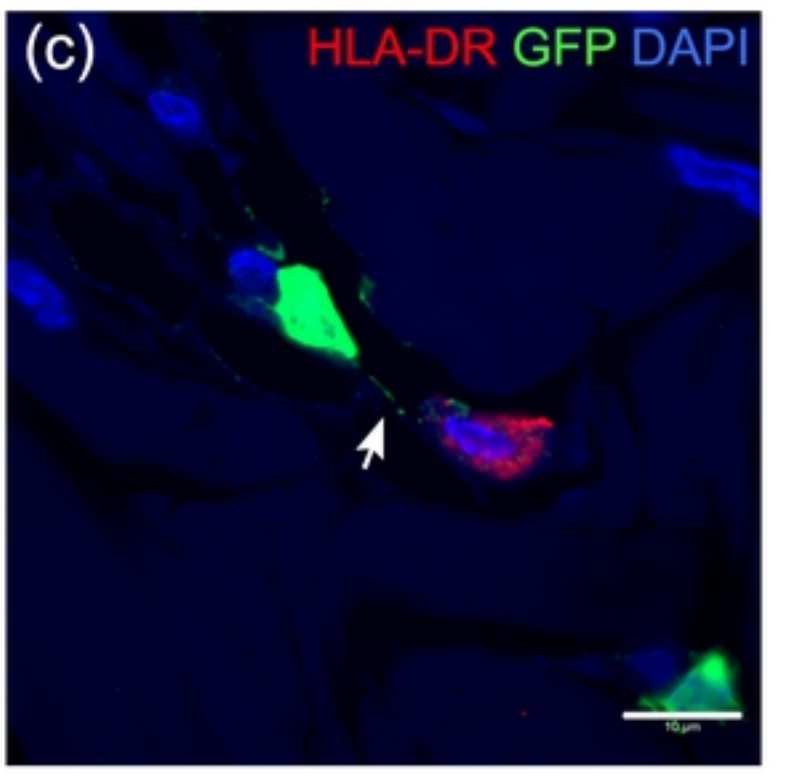

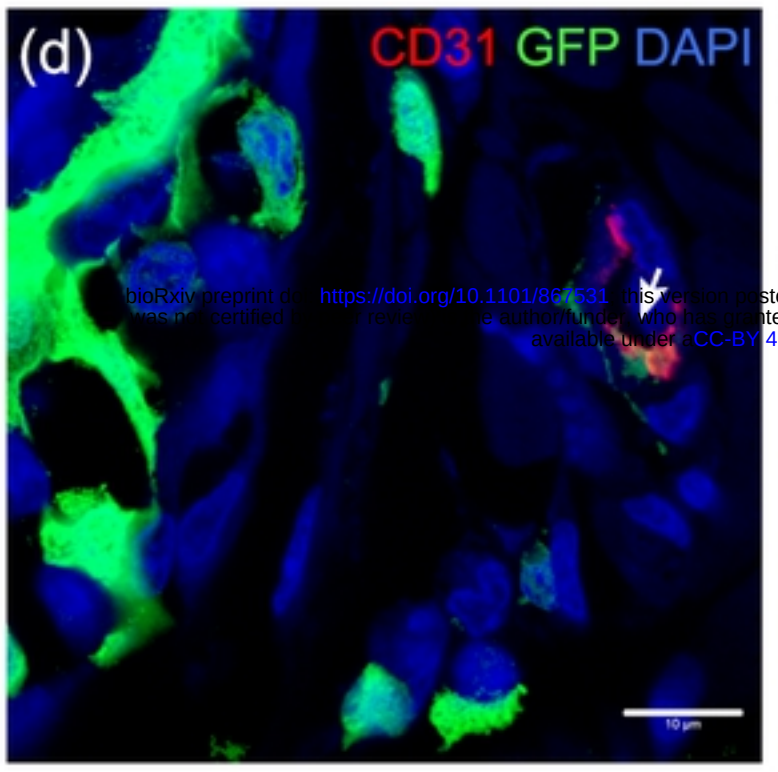

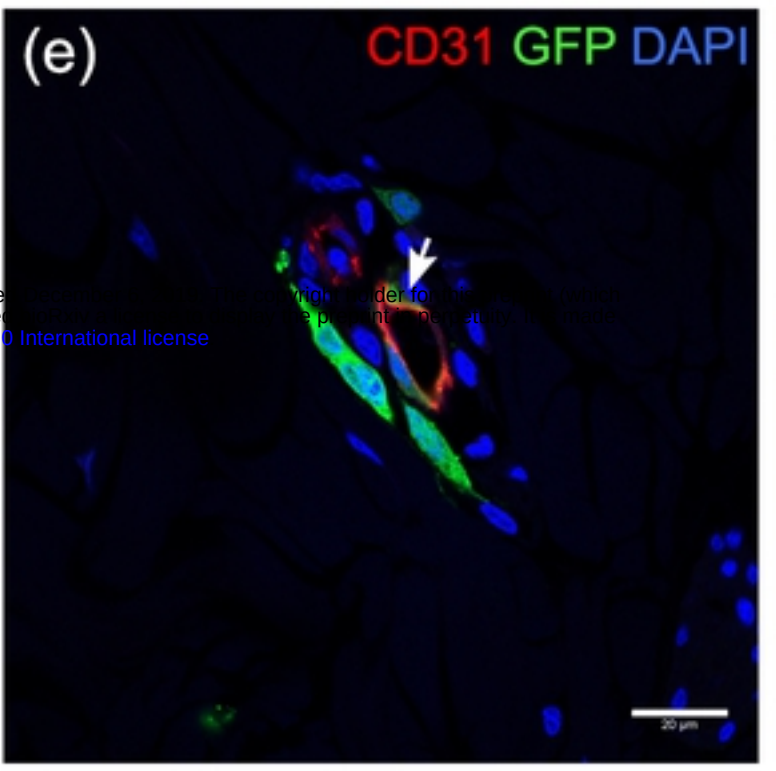

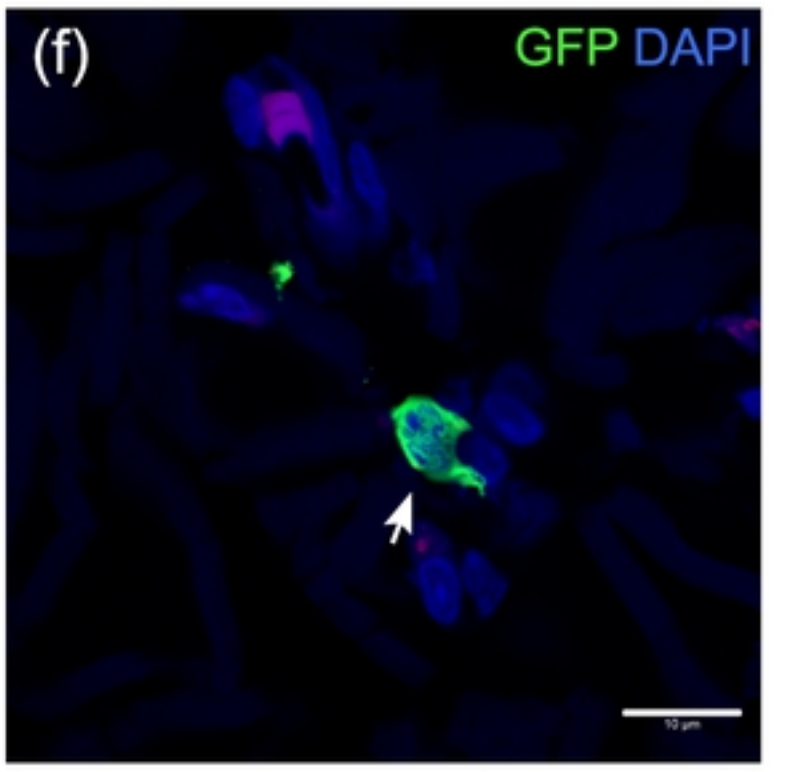

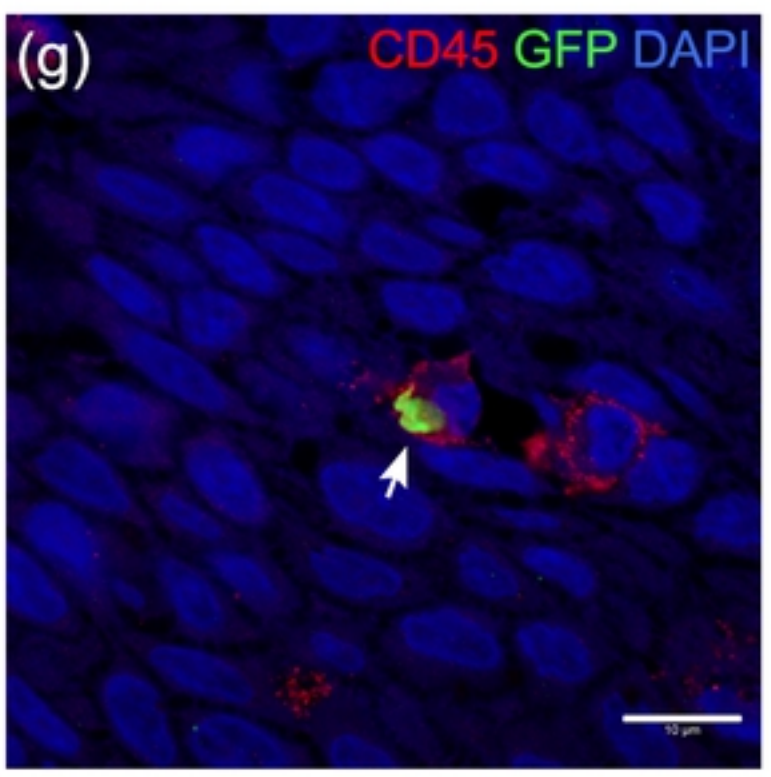

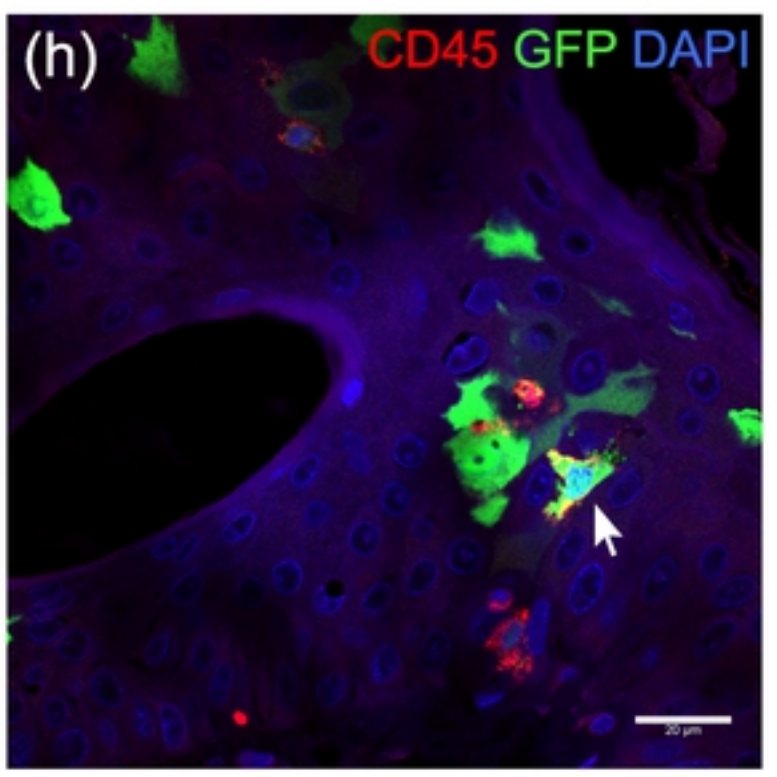

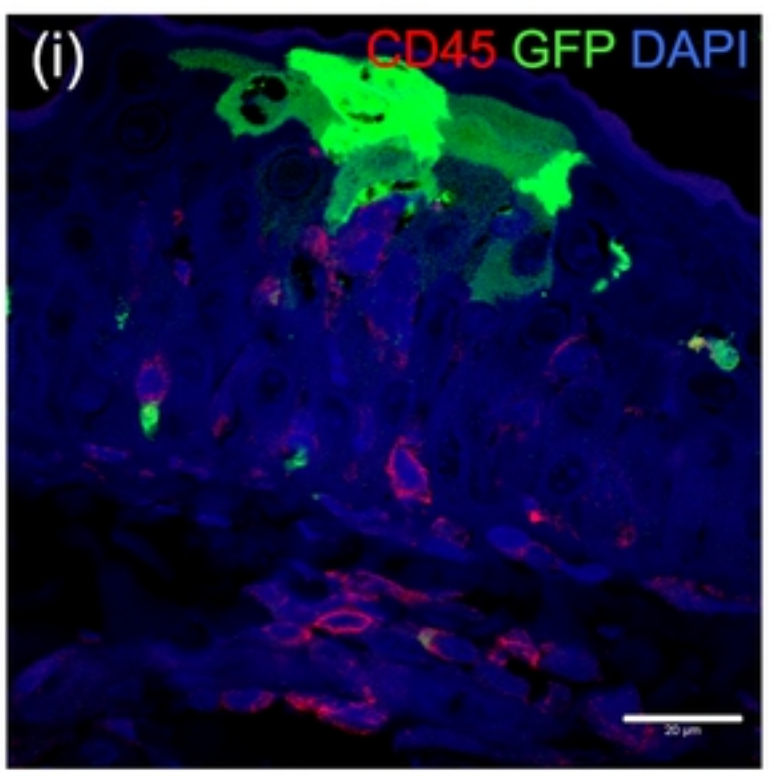

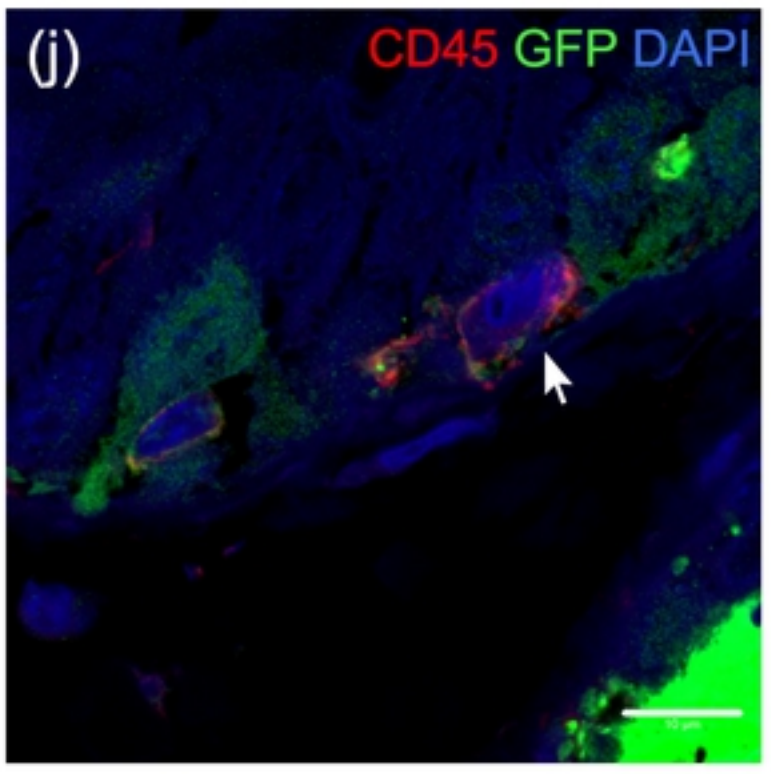

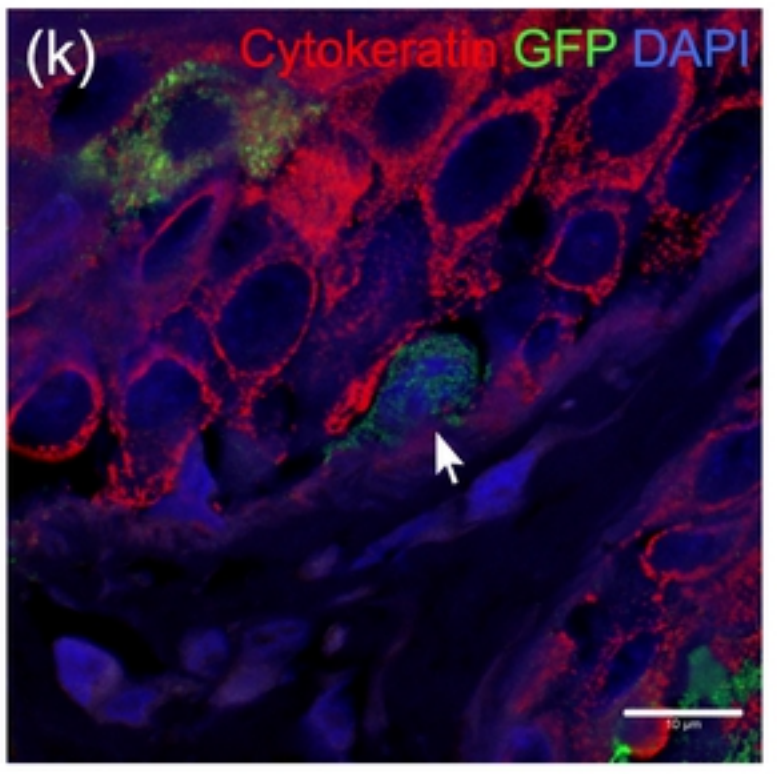

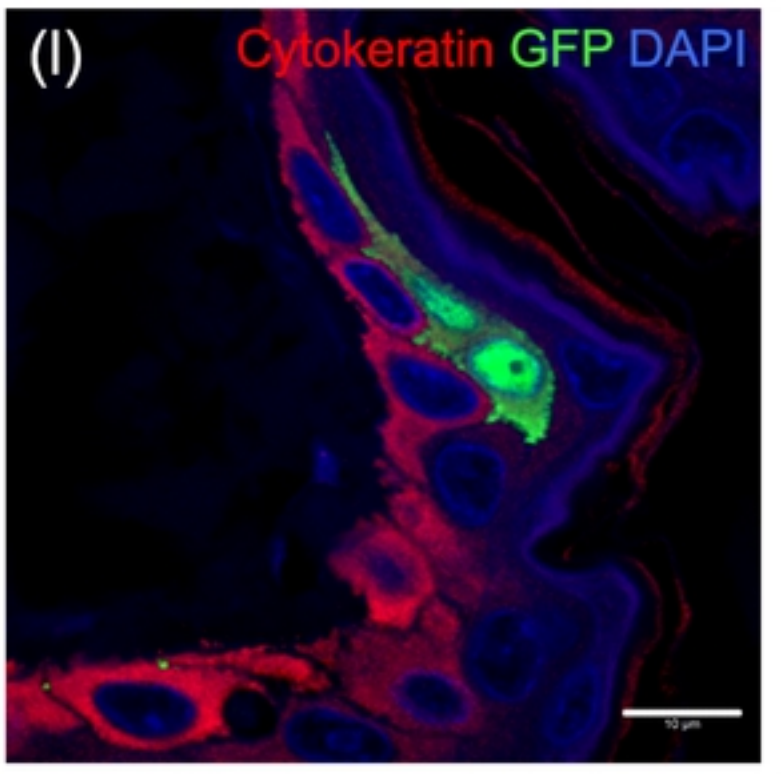

Figure 4

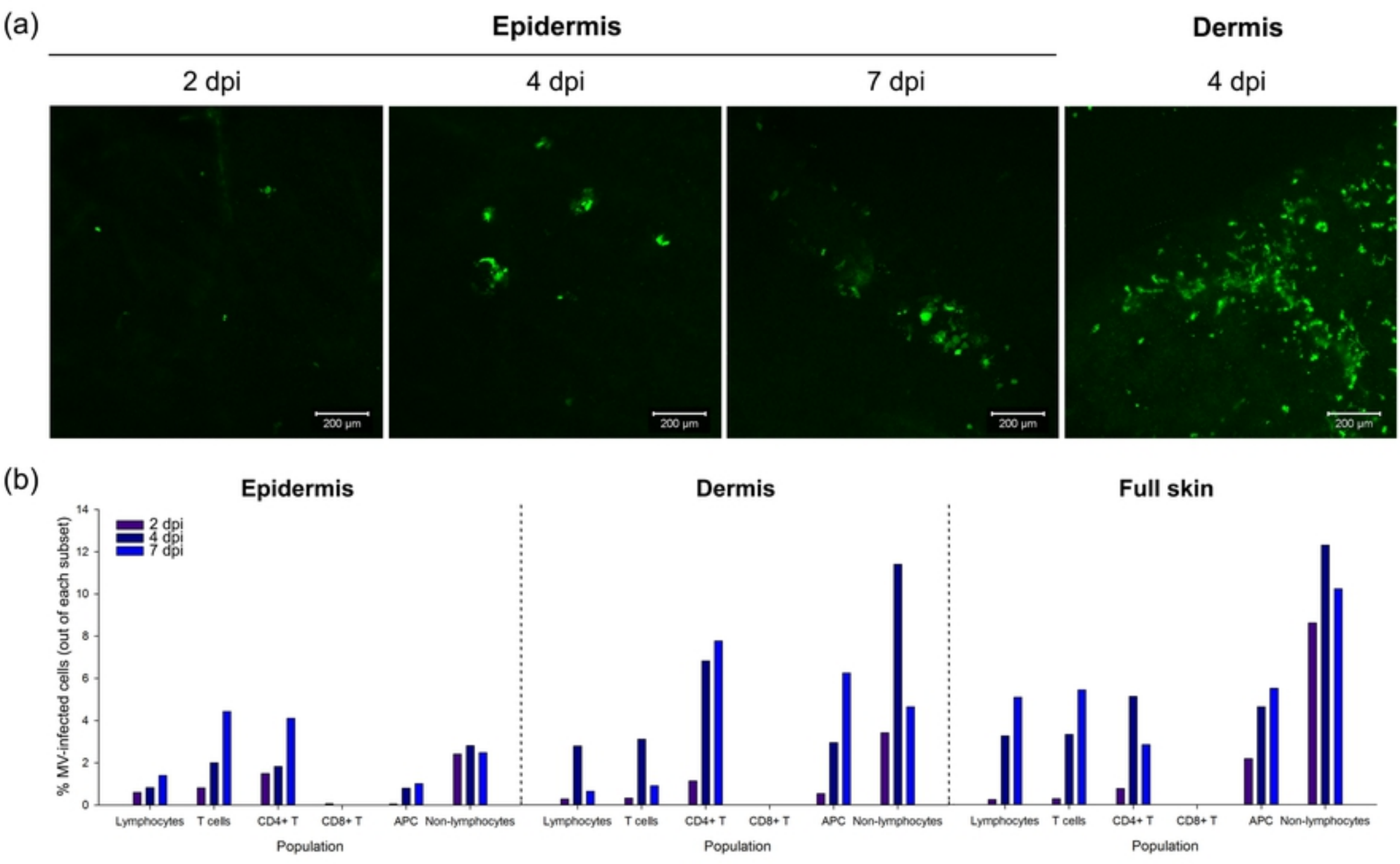
(a)
Epidermis
Dermis
2 dpi
4 dpi
7 dpi
4 dpi
200 µm
200 µm
200 µm
200 µm
(b)
Epidermis
Dermis
Full skin
2 dpi
4 dpi
7 dpi
% MV-infected cells (out of each subset)
0
2
4
6
8
10
12
14
Lymphocytes
T cells
CD4+ T
CD8+ T
APC
Non-lymphocytes
Population

Figure 5

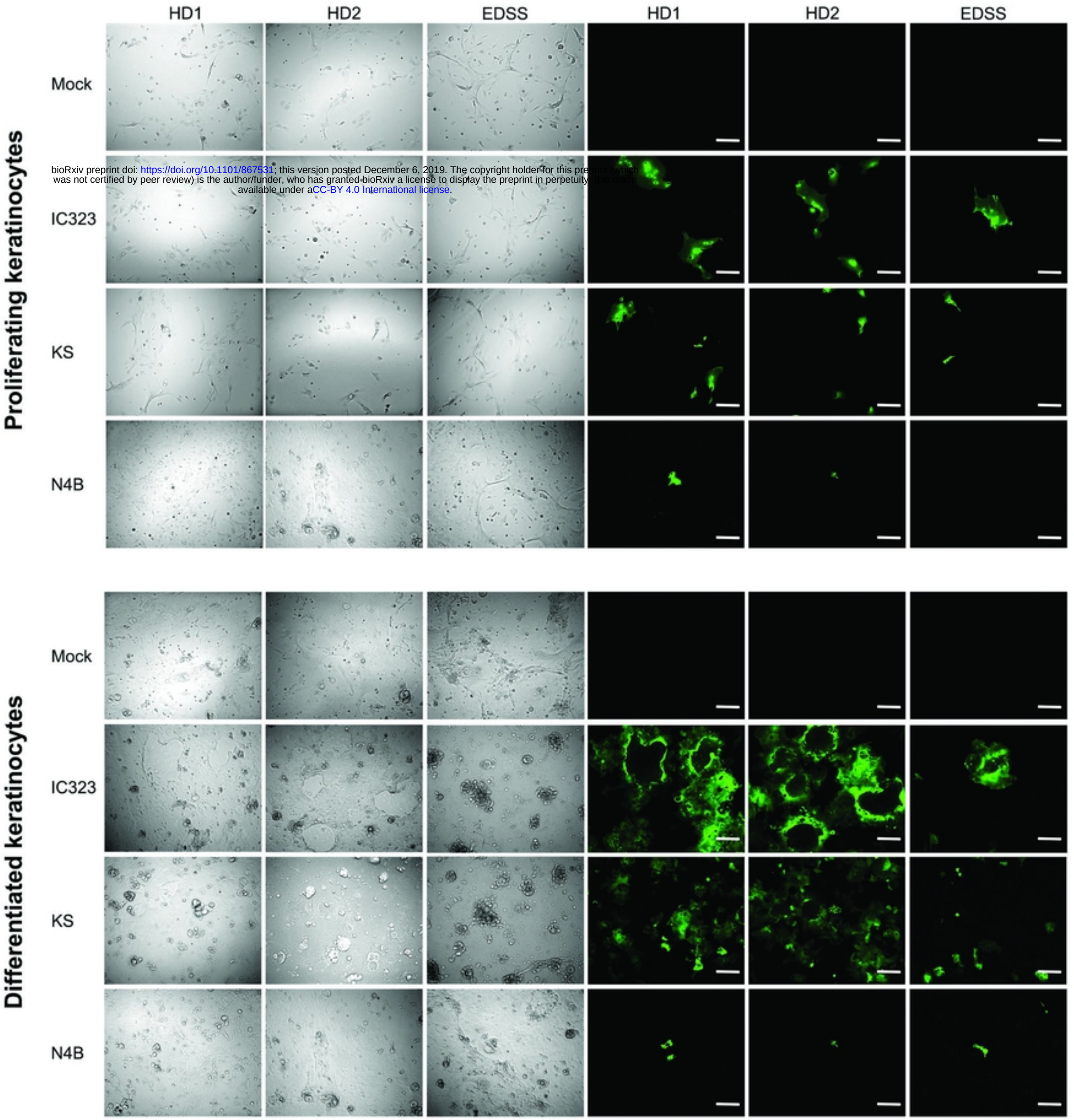

Figure 6

(a)

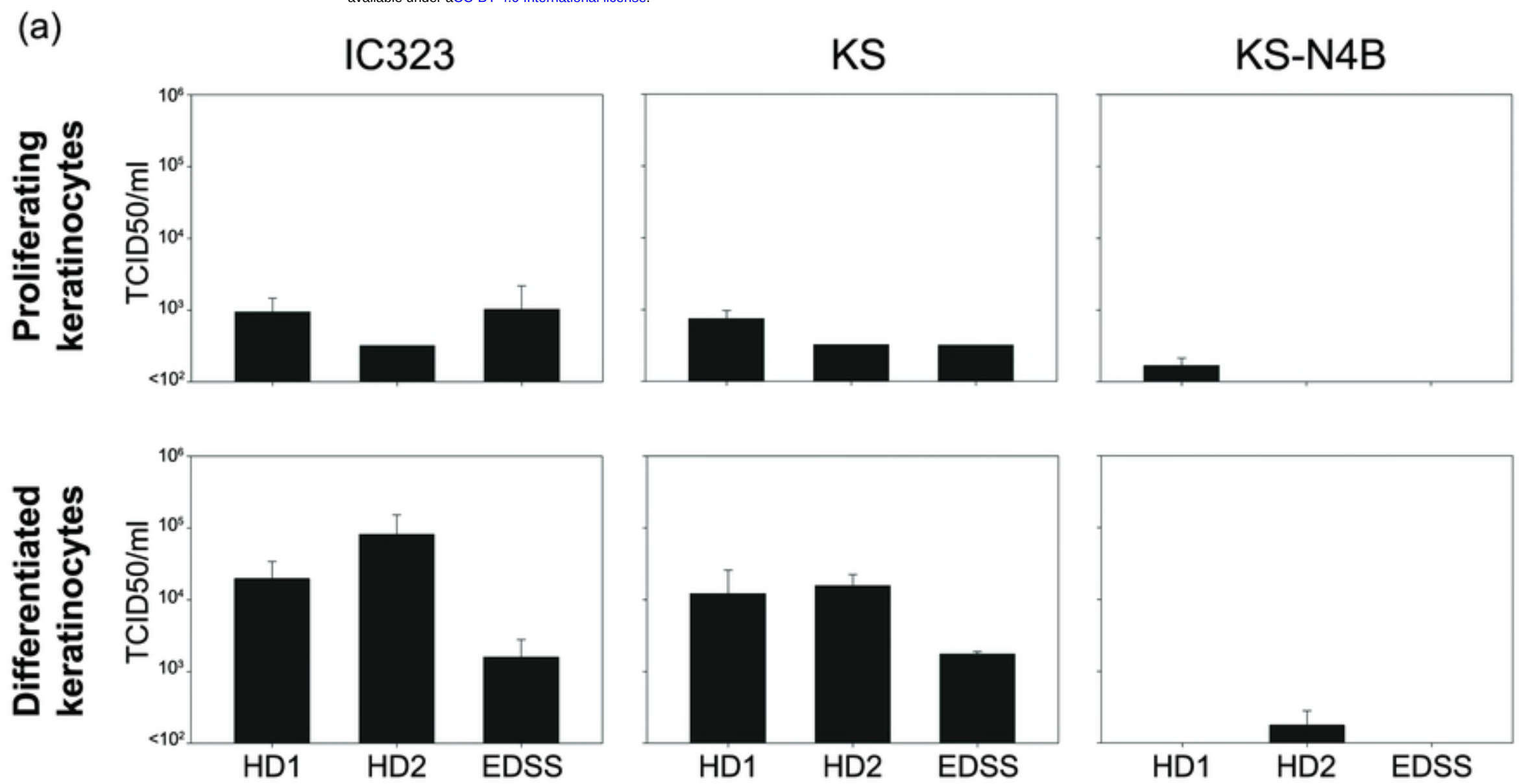

(b)

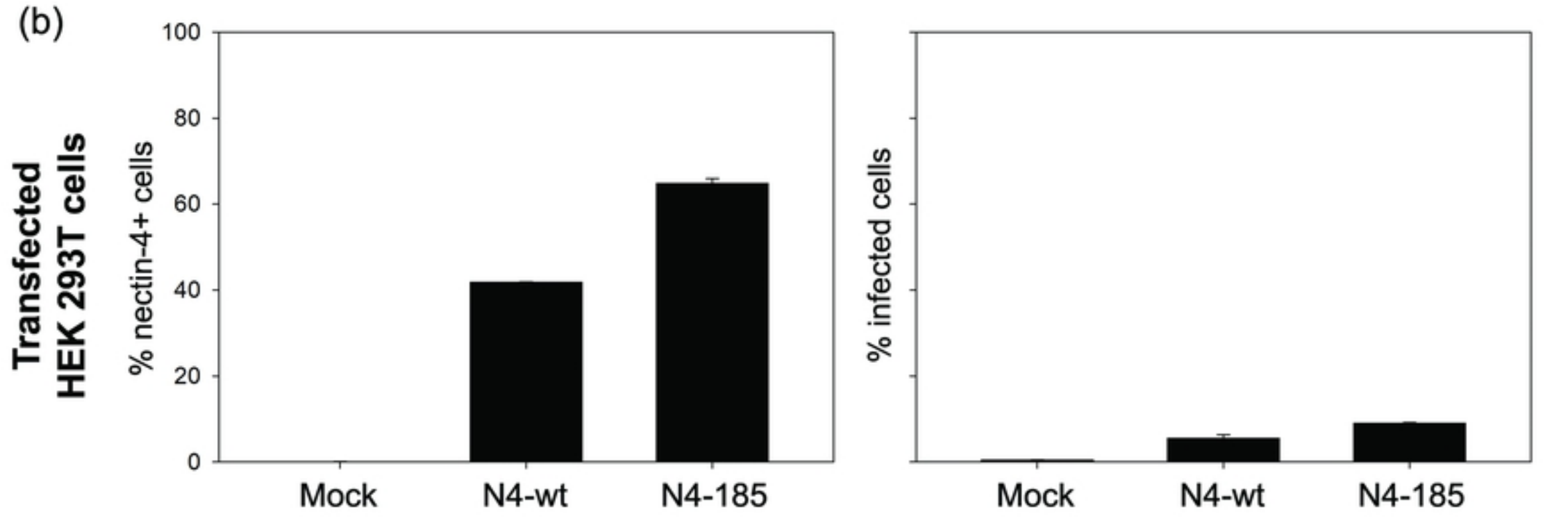

Figure 7

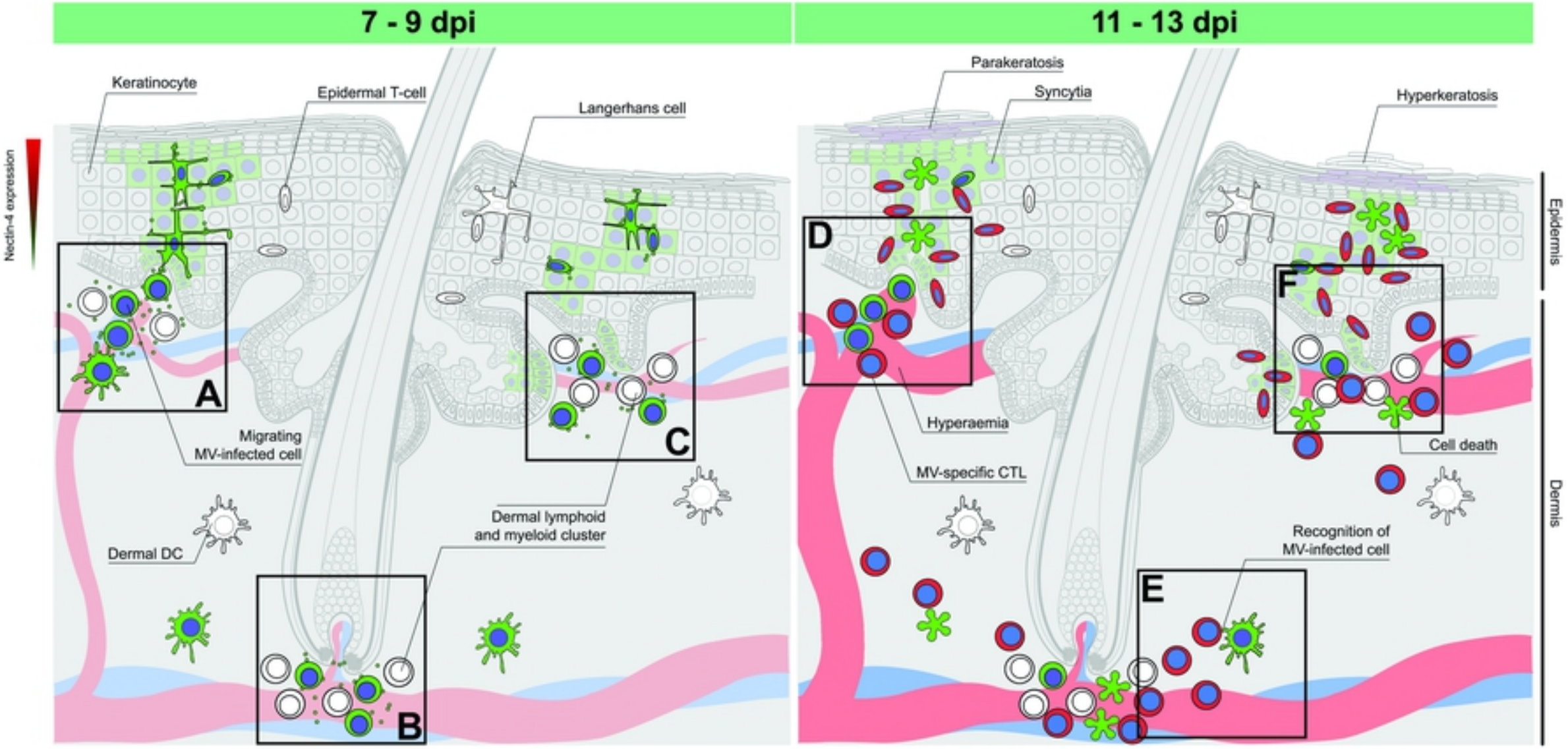
7 - 9 dpi
11 - 13 dpi
Nectin-4 expression
Keratinocyte
Epidermal T-cell
Langerhans cell
Migrating
MV-infected cell
Dermal DC
Dermal lymphoid
and myeloid cluster
A
B
C
Parakeratosis
Syncytia
Hyperkeratosis
D
Hyperaemia
MV-specific CTL
F
Cell death
Recognition of
MV-infected cell
E
Epidermis
Dermis

Figure 8